Master Dissertation in Mechanical Engineering

A three-station creep machine for adhesive joints: testing and characterization

Author:
Gonçalo Noutel Fontes Ferreira Bezerra

Supervisor:
António M.F. Mendes Lopes
Co-Supervisors:
Lucas F. M. da Silva
Carlos M.S. Moreira da Silva

Integrated Master in Mechanical Engineering

February, 2021

Acknowledgements

Em primeiro lugar, e acima de tudo, aos meus pais que foram sempre a luz da minha vigília. Aos meus avós, pelo carinho, preocupação e conselhos inesgotáveis ao longo de todo este percurso.

Aos meus orientadores, professor António Mendes Lopes, professor Lucas da Silva e professor Carlos Moreira da Silva, agradeço a constante disponibilidade, a experiência e conhecimento que partilharam, as críticas construtivas e a atitude de que é sempre possível elevarmo-nos e ao nosso trabalho.

A todos os do Grupo AJPU, obrigado. Pela disponibilidade, pela entreajuda, por todo o acompanhamento e conselhos que me guiaram durante e na conclusão da minha dissertação.

Um especial obrigado ao Sr. Joaquim que dispôs de grande parte do seu tempo para me apoiar e partilhar consigo a sua inesgotável experiência. Sem ele, todo o processo seria extremamente árduo, sendo outra figura incontornável no desenvolvimento desta dissertação.

Aos amigos que partilharam, de perto, esta viagem comigo, oriundos de todo o lado e de lado nenhum, apraz-me confessar que foram um dos acasos mais felizes neste caos probabilístico que é a vida. Permitiram-me edificar uma segunda casa onde morei com todos vocês, aprendendo que algumas pessoas são a nossa casa e nelas moramos para sempre.

Resta-me agradecer aos amigos com quem partilho a vida há mais tempo, parece agora desde sempre. Ainda que não tão presentes tenham estado neste ciclo, são peças imutáveis de uma vida que sem eles, se torna fraturada. Um deles disse-me uma vez "Há amores que não morrem nunca". Assim espero.

Obrigado.

Abstract

Adhesive joints offer several advantages over conventional fixing methods. Although there is an exponential growth in its use in various industries (especially automotive), the knowledge and study of adhesive joints is still somewhat limited.

The main objective of FEUP's Adhesive Group (AJPU) is the study and characterization of various types of adhesives and adhesive joints. The characterization of the behavior of adhesives and adhesive joints when subjected to creep conditions is still somewhat scarce. AJPU has several testing equipment, some of which have the ability to perform creep tests. However, such tests are continuous and long, which occupies the equipment that are necessary for the execution of other tests. The Group still lacks a specialized and dedicated machine to only study the behavior of adhesives and adhesive joints under creep conditions.

The objective of this dissertation is to continue the previous work of Freire, Pina e Silva in the development of a creep testing machine with three stations, allowing them to work independently and simultaneously in the execution of tests on adhesive joints as well as in the acquisition of data from those same tests.

First, the mechanical components and the pneumatic and electrical circuits were overhauled, followed by necessary adjustments for the system to become fully functional. After this hardware revision, software was developed in a way that allows all stations to exhibit a very similar, albeit independent, behavior, presenting the ability to exert a constant force between 100 N and 2800 N on the specimen, while recording, at regular intervals, the values of the load exerted and the displacement caused by that load. This registration of values can be subsequently processed automatically, facilitating the analysis process.

The software was tested multiple times to ensure that the processes were repeated in a constant and predictable manner. All the hardware was also tested, allowing to correct and adjust values from the analog signals of the transducers. Further tests have been carried out to ensure correct functioning during a creep test.

Finally, creep tests were performed on the machine and compared to each other, with another machine and with previous studies, allowing to draw conclusions about the performance of the machine, especially in terms of repeatability, accuracy and reliability in the results obtained and to validate the machine that is the main objective of this dissertation.

Resumo

As juntas adesivas oferecem diversas vantagens em relação aos métodos de fixação convencionais. Apesar de se verificar um crescimento exponencial na sua utilização em várias indústrias (especialmente automóvel), o conhecimento e estudo de juntas adesivas é, ainda, algo limitado.

O principal objetivo do Grupo de Adesivos (AJPU) da FEUP é o estudo e caracterização de vários tipos de adesivos e juntas adesivas. A caracterização do comportamento de adesivos e juntas adesivas quando sujeitas a condições de fluência é ainda algo escassa. A AJPU possui vários equipamentos de teste, sendo que alguns têm a capacidade de executar testes de fluência. Contudo, tais testes são contínuos e longos, o que ocupa esses equipamentos que são necessários para a execução de outros testes. O Grupo ainda carece de uma máquina especializada e dedicada para somente estudar o comportamento de adesivos e juntas adesivas em condições de fluência.

O objetivo desta dissertação é continuar os trabalhos anteriores de Freire, Pina e Silva no desenvolvimento de uma máquina de ensaios de fluência com três estações, permitindo que estas trabalhem de forma independente e em simultâneo na execução de testes a juntas adesivas bem como na aquisição de dados provenientes desses mesmos testes.

Primeiramente, os componentes mecânicos e os circuitos pneumático e elétrico foram revistos, seguidos de ajustes necessários para que o sistema se tornasse totalmente funcional. Após essa revisão de hardware, desenvolveu-se o software que permite a todas as estações apresentar um comportamento muito semelhante, ainda que independente, apresentando a capacidade de exercer uma força constante compreendida entre 100 N e 2800 N sobre o provete, enquanto regista, a intervalos regulares, os valores de carga exercida e de deslocamento provocado por essa carga. Esse registo de valores é posteriormente processado automaticamente, facilitando o processo de análise.

O software foi testado múltiplas vezes para assegurar que os processos se repetiam de forma constante e previsível. Todo o hardware foi também testado, permitindo corrigir e ajustar valores provenientes dos sinais analogicos dos transdutores. Outros testes foram realizados para assegurar o funcionamento correto durante um teste de fluência.

Por fim, testes de fluência foram executados na máquina e comparados entre si, com outra máquina e com estudos prévios, permitindo tirar conclusões sobre a performance da máquina, especialmente em termos de repetibilidade, exactidão e segurança nos resultados obtidos e validar a máquina que é o principal objetivo desta dissertação..

"Few men have imagination enough for reality."

Johann Wolfgang Von Goethe

Contents

List of Figures

List of Tables

Chapter 1
Introduction

1.1 Background and Motivation

Adhesives are increasingly being used in a wide range of industries such as automotive, aerospace and aeronautical due to their low weight, which allows a lower energy consumption, along with less emissions [1].

Adhesives are also used because of their unique advantages when compared to conventional mechanical joining methods. Among those advantages are a more uniform stress distribution, which leads to a good resistance to dynamic fatigue, higher stiffness and load transmission, the ability to bond dissimilar materials and thin sheets of material, the possibility of process automation, design flexibility and regular contours [2].

However, the development of the adhesives field and their integration in industry is far more recent than conventional mechanical joints. In an ever growing field, further studies are crucial for assessing the behaviour of the material.

AJPU (Advanced Joining Process Unit) is a group of researchers based in FEUP (Faculdade de Engenharia da Universidade do Porto) dedicated to study the properties and behaviour of adhesives and adhesive joints. AJPU is involved in various projects, therefore there is a need of various machinery. Although, AJPU already is in possession of a machine capable of performing creep tests, that machine is required to perform another tests for different projects and creep testing can demand several hours, days or weeks of continuous use. Also, even if that machine was used for creep testing, it could only perform one test at a time.

A three-station creep machine for adhesive testing alone able to provide reliable test results is of added value to AJPU.

1.2 Objectives

The main objective of this dissertation is to continue developing the three-station creep machine for adhesive joints and validate the results of the creep tests performed by the machine.

The first step was to assess the state of the machine by studying the previous work done by Freire [3], Pina [4] and Silva [5].

During a creep test, the machine should be able to exert a constant load between 100 N and (almost) 3000 N over a bulk or single lap joint specimen mounted in the machine's mechanical grips, while the displacement of the specimen, limited by the travel extension of about 250 mm (limited by the positioning of the mechanical grips), is occurring.

The machine has three stations that should share the above mentioned behaviour while working independently yet simultaneously. All the data from said tests should be recorded and stored for further analysis.

Regarding the validation of the creep test results, the first objective is to ensure that all the hardware components are working properly and the acquisition systems are calibrated as well as ensuring the software is functioning as desired.

Finally, this dissertation aims for the validation of the machine itself, meaning the machine performs accurate and repeatable creep tests.

1.3 Methodology

Initially, a literature review about creep test machines was conducted. At the same time, the previous work done on the machine by Pina and Silva was studied and analyzed, to assess the developing state of the machine.

After understanding the previous work, the overall state of the machine was revised. This meant analyzing the mechanical design, and the electrical and pneumatic circuits. The pneumatic circuit was rearranged, some missing elements of the electric circuit were manufactured while others replaced or repaired until all the hardware was fully functional.

Then, the three-station creep testing machine software was structured and fully developed, allowing the three stations to have a similar behaviour and performance while working independently and simultaneously.

The hardware, specially the transducers' systems and the pressure regulating system were tested and validated, ensuring an accurate measuring of the load, displacement and pressure.

The machine was also tested regarding the capability to maintain a constant load applied to the specimen over long periods of time and regarding the influence that the stations exerted on one another in terms of pressure.

At last, creep test were conducted and compared to tests executed on another machine and to previous test results described on papers to assess the accuracy of the results and validate the overall performance of the machine.

1.4 Dissertation Outline

This dissertation is organized in seven chapters.

The first one contains a brief introduction to the project, describes the structure of this dissertation and the objectives this dissertation aims for.

The second chapter covers a literature review about adhesives, creep testing, commercial creep machines and NI's software LabVIEW.

The third chapter addresses the physical components of the machine and it is divided in three parts, each covering a system of the machine: the mechanical design, the pneumatic circuit and the electric circuit.

The fourth chapter explores the software development for the automation and control of the three-station creep machine.

The fifth chapter covers the testing and validation of the software and hardware components of the system.

In the sixth chapter, creep tests are examined, evaluating the performance of the machine.

The seventh chapter contains the most relevant conclusions of the dissertation and suggests improvements to enhance the performance of the machine as a whole.

Chapter 2
Literature Review

This chapter contains a brief literature review that addresses adhesives, creep tests, the creep specimens used on those tests, the standard commercial machines used for creep testing as well as the software to display and record the test data.

2.1 Adhesives

Adhesion is a phenomenon defined as the attraction of two different substances resulting from intermolecular forces between them [6].

Adhesive is defined as a substance capable of holding at least two surfaces in a strong and permanent manner. Adhesives are chosen because of their holding and bonding power. They are generally materials having high shear and tensile strength. Throughout History many natural substances were used as adhesives like skin, milk, beeswax, wet lime, glue and chalk. In the twentieth century, the real development of the adhesive industry started with the polymeric and elastomeric resins [7].

Adhesives joints can provide some advantages when compared with the mechanical ones. They have the ability to joint a myriad of unalike surfaces like metal and metal, metal and glass, metal and plastic and plastic and plastic [7]. To bond thin sheets over large areas leading to lighter and stronger assemblies that could not have been achieved with mechanical fastening is a huge point of interest in the current industry . They have better stress distribution, increased stiffness and resistance to fatigue and vibration damping. Adhesives can provide the same structural strength as conventional assemblies at lower weight and cost - good strength to weight ratio [1].

However, some downsides cannot be ignored. Firstly, adhesives are usually limited by their service temperature. Secondly, they can be susceptible to high humidity environments. Also, they require more caution in preparation of the surfaces about to be bonded and the adhesive can only be applied in clean, plain surfaces. The curing process is not instantaneous meaning the full strength of the adhesive is not developed immediately. Lastly, adhesives' shear strength and toughness is lower than those of metals and they are not indicated for joining thick metallic surfaces [8].

2.2 Creep

Creep is the increase in strain or deformation of a material (or structure) over a period of time when the material is subjected to a constant load at constant temperature for an extended period of time [9]. Therefore, it is a time and temperature dependant phenomenon (Figure 2.1). Unlike metals,where creep usually occurs at high temperatures, adhesives, where the creep response is the result of the time-dependant untangling of the polymer chains, can undergo creep deformation at room temperature (referred as cold flow) as well as at low stress levels (well below the yield point of such material) [7]. Since this factors can lead to a considerable reduction in life expectancy of the component, performing creep tests in order to determine a material's expected behaviour under certain operation or environmental conditions is of crucial importance.

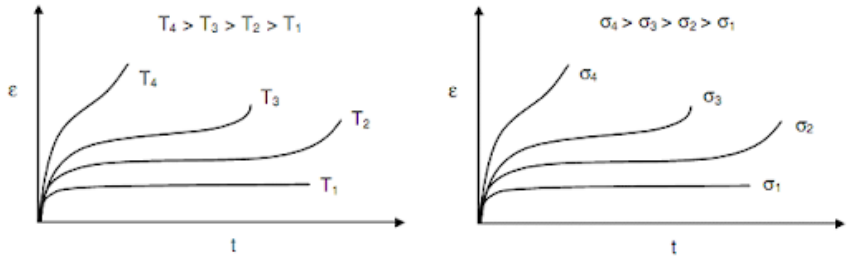

Figure 2.1: Influence of Load and Temperature in creep phenomenon

A creep test is performed by submitting the specimen to a constant tensile or compressive load (generally below the load required to break the bond) at a constant temperature during a prolonged elapsed time, in order to measure the deformation of the adhesive. While testing, the material's deformations is recorded at specific time intervals and the overall data recorded is plotted. Usually, creep data is presented as a plot of creep compliance versus time, at a constant stress and temperature levels (maintaining a constant temperature during a creep test is critical due to possible thermal expansion or shrinkage of the material) [1].

A usual creep response exhibits three distinct phases after the initial elastic strain, as shown in Figure 2.2. The first stage, called primary creep, exhibits a decreasing creep rate. The speed of deformation decreases because at this stage the creep resistance increases due to the deformation itself. Then, the second stage, also known as secondary creep, begins, in which the creep rate is approximately constant. Due to the balance between the hardening and restoration phenomenons, this stage presents the slowest creep rate during the test - the minimum creep rate or steady-state creep rate. Finally, the specimens enters in the third stage, the tertiary creep, where the deformation rate rises continually until the rupture of the specimen. This event is called creep rupture and is measured by the time to fracture [9].

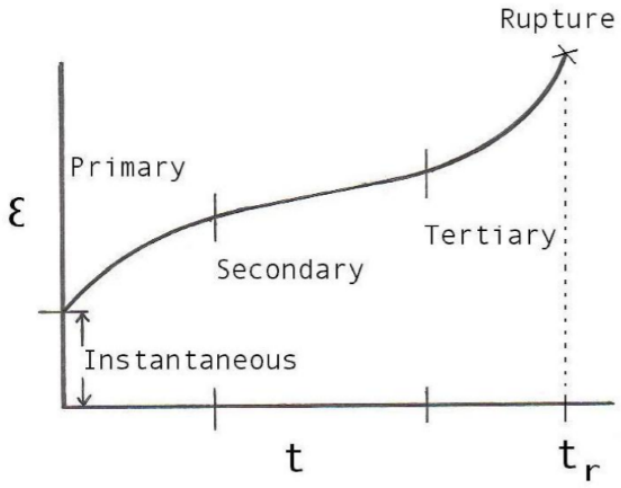

Figure 2.2: The three stages of creep behaviour

Creep is the technical parameter that addresses the question of what happens to the adhesive after its application. It characterizes how a material flows or changes shape under load. The common expectation is that an adhesive will hold its position after application as the curing process takes place. The reality is that mechanical forces, due either to gravity or to the way in which the mating surfaces come together, can cause movement of the adhesive material. Ideally, manufacturers evaluate adhesive material for this behavior and quantify the creep property for a given application [10].

2.3 Creep test specimens

Several types of specimens with different geometries can be used when performing a mechanical test. However, when performing a creep test the usual specimens are either bulk specimens or single lap joint specimens.

Bulk specimens typically consist of a waisted section with parallel sides ("dogbone" specimen), as shown in Figure 2.3. Bulk adhesive's properties are intrinsic to the adhesive and not influenced by the adherents. They are usually produced by pouring or injecting the adhesive (which can be mixed with an hardener) into a mould and cured after. This kind of specimen, also standard in plastic materials testing, is easy to perform tests with. Also, the data relative to the test is relatively straightforward to analyze [11].

Figure 2.3: Bulk specimen

Single lap joints are easy to manufacture and represent the most common joint configuration (Figure 2.4). The adhesive layer that binds the two materials, when tested is under a constant state of stress. Since this configuration resembles the most the practical applications due to the small thickness of the adhesive or the thin sheets of adherent, testing using single lap joints can provide data which can be used in different industries [11].

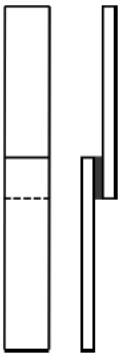

Figure 2.4: Single lap joint specimen

2.4 Commercial Creep test machines

When designing a machine or a product it is mandatory to investigate the market to evaluate the solutions that are currently offered. Doing so, it is notorious the lack of systems available purposefully designed for creep testing, not to mention adhesive creep testing.

The solutions offered for creep testing are mainly UTMs - Universal Testing Machines. These machines are able to perform a myriad of tests: tensile, compression, bend, peel, tear, etc. In other words they are very versatile. Since creep tests can be considered tensile tests, these machines can be used to perform creep tests. However, being universal testing machines means not

only they can perform several mechanical tests, but also that they are used to test many materials. This factor translates into the existence of applied load ranges much higher than those required to perform a creep test.

INSTRON, one of the reference manufacturers of UTMs, has a broad catalog of this type of machinery. Despite such variety being significantly reduced when searching for multi-station universal testing machines, INSTRON still can provide such system: the 5900 Series Multi-Station Test Frame for Simultaneous Mechanical Testing (Figure 2.5). [12]. This model provides:

- 3 or 5 independent stations;
- Total load capacity of 30 kN;
- Crosshead travel of 1140 mm or 1640 mm;
- Pneumatic side-acting grips;
- Environmental chamber providing temperatures between -40°C and 200°C;
- Bluehill Universal test control software;

Although the total load capacity of the machine is 30 kN, this available load is divided by the number of stations or load strings available. This means that a 3 station system will provide 10 kN per load string and a 5 station system will provide 6 kN per load string.

Figure 2.5: INSTRON's multi-station UTM [12]

Bluehill Universal test control software complements the physical structure of the machine and presents some interesting features (Figure 2.6) [13]:

- Live display of force, displacement and time;
- Graphs displaying force vs. displacement data, stress vs. strain data or displacement vs. time data;
- Results table that allow sorting results by different parameters;
- Specimen selector to manage a specific test and quickly analyze the results;
- Simple interface for the user;

Figure 2.6: Bluehill software interface [13]

Zwick Roell, another known manufacturer of UTMs, commercialize a model designed specifically for testing creep behaviour in plastics and polymers: the Kappa Multistation Creep Testing Machine (Figure 2.7) [14]. This eletromechanical testing machine offers individually controlled load axis. Also, similarly to INSTRON's model, it is very versatile, allowing not only the performing of creep tests but also relaxation tests and can be used to test the creep phenomenon on other materials. The Kappa model by Zwick Roell provides:

- 5 (or 6 if required by the costumer) independent test axes;
- Maximum of 10 kN applied load per axis;

- Crosshead travel of 200 mm;
- Long-term tests up to 10,000 h;
- Temperature chamber accommodating temperatures ranging from -70°C to 250°C;
- Monitoring and analysis of test results through testXpert III Multistation software

Figure 2.7: Zwick Roell multistation creep testing model [14]

Although the mechanical design of the machine is very standard and similar to INSTRON, the software system, despite providing the same or identical features, and mainly the interface is where some differences surface.

TestXpert III Multistation software [15], described by Zwick Roell as one of the most reliable testing software in the market, flexible and efficient, exhibit some particular solutions (Figure 2.8):

- Intuitive and work-flow based (setup, test configuration, test run, results display);
- Intelligent wizard (shows what test parameters are not yet defined and if they are plausible);
- Test using superimposed multi-axis solutions with only one testing software;
- Analyze specimen behaviour with a real-time view of the test sequence or using online calculation of test results.
- Reliable data import and export;

- Safety tools for protecting test results from manipulation
- traceability in test results;

Figure 2.8: TestXpert III Multistation software[15]

This two brands above exposed are the standard when it comes to UTMs. However, AJPU is only interested in testing adhesives and adhesive joints, and the load range of these machines is higher than necessary. Also, these machines tend to be very expensive. For those reasons, APJU is interested in developing their own multi station creep machine.

Chapter 3
Machine Overview

In previous works, all the hardware present in the three-station creep machine were thought, chosen and assembled. This chapter will briefly expose the design of the machine. More specifically, it will provide an description of the mechanical design and assembly and the pneumatic and electric circuits.

Although the conceptual design of the physical parts of the machine is prior to this dissertation, it is relevant to understand the software behaviour that was implemented, what hardware is being controlled and how the system functions as a whole.

3.1 Mechanical Design

In the present sub chapter, a summary of the machine designed by Freire [3] and Pina [4] and revised by Silva [5] will be provided.

The machine designed for creep testing must be able to endure maximum loads applied, suffering little to none deflection as well as being perfectly aligned in order to provide reliable data of the creep tests performed.

Analyzing the Figure 3.1, one can notice that the machine consists of three equally design, identical stations.

Each station can also be divided into its lower assembly (3) and upper assembly (2). The lower assembly contains the pneumatic cylinder and its connections to the lower grips and to the lower beam. The upper assembly consists of the upper grip and the load cell connected by the upper coupling ending in an axial spherical plain bearing.

The mechanical structure (4) contains the Load Frame formed by an upper beam and a lower beam connected by two columns that are subjected to the test conditions, and the Support Frame that supports the whole machine. The Load Frame is assembled directly on top of the Support Frame.

The mechanical wedge grips (1) - two per station, six in total - have an important function: they are the ones responsible for tightening the specimen and holding it in place while the the specimen is being subjected to the applied load during the creep test. The grips (Figure 3.2) are 254 mm apart when the cylinder is in its lower position.

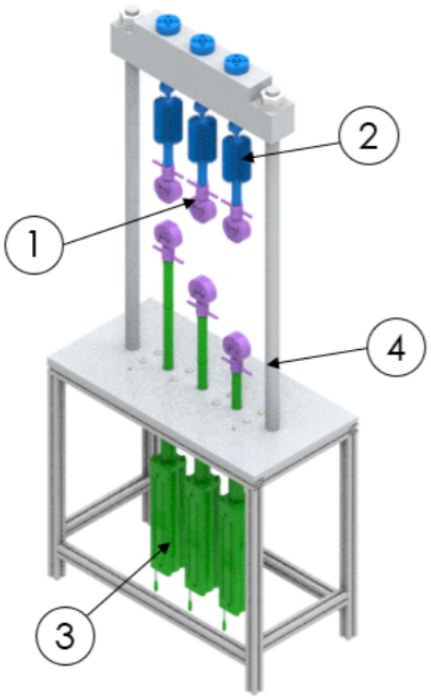

Figure 3.1: Creep test machine design [4]

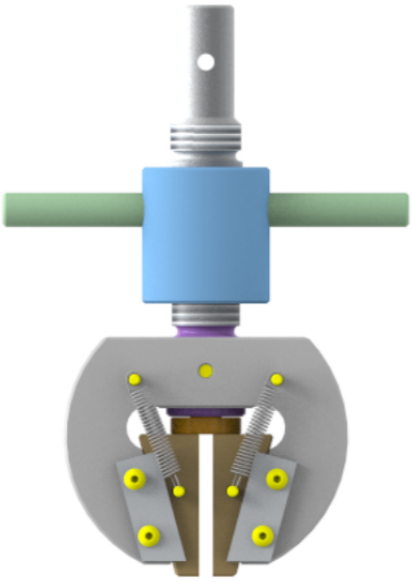

Figure 3.2: Mechanical action wedge grip [4]

3.2 Pneumatic Circuit

The pneumatic circuit's function is to supply airflow for the moving of the lower assembly and its grip to the intended position before the commence of the creep test. During the creep test, it must supply airflow to the upper

chamber of the cylinder in such way that allows a constant load applied to the specimen that is being tested.

Having that specifications in mind, the pneumatic circuit has been assembled (Figure 3.3). This circuit contains an air treatment unit (1), a 5/3 directional valve with closed center (2), a pressure regulator valve (3), a cylinder (5) prepared to the instalment of two proximity sensors (6) and two flow control valves (4). The numbers inside parenthesis refer to the identification of the components of the pneumatic circuit present in Figure 3.3. The pneumatic circuit described is for one station only because all of the stations have an identical pneumatic circuit downstream of the air treatment unit.

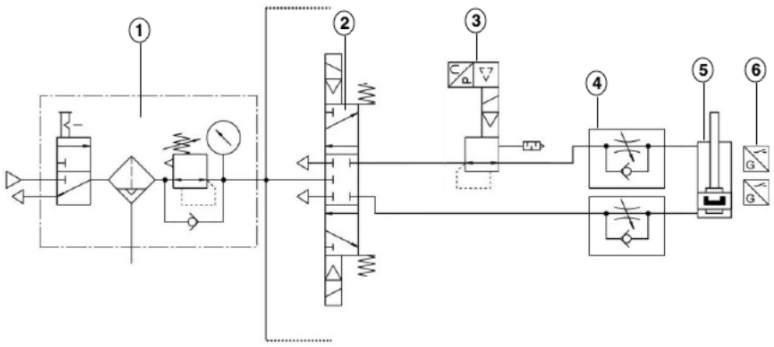

Figure 3.3: Station pneumatic circuit

The VPPX pressure regulator valve is downstream of the directional valve, meaning it only regulates the pressure of the upper chamber (responsible for the descent of the cylinder). Perhaps, the pressure regulator valve should be upstream of the directional valve, being able to regulate both chambers. However, by adjusting the flow control valve of the upper chamber and restraining the exiting airflow, it is possible to regulate the ascension speed of the cylinder. Since during the creep test the cylinder is moving down, that is the movement that is crucial to regulate and control and for that reason the VPPX was inserted after the directional valve, controlling just the airflow allowed into the upper chamber.

All the components of the pneumatic circuit will be succinctly described in the following subsections.

3.2.1 Cylinders

The cylinders acquired and present in the machine are three pneumatic cylinders FESTO Q-80-300-QA [16], meaning these cylinders have a 300 mm work stroke and a 80 mm diameter piston (Figure 3.4). Moreover, it also has a protection against rotation: a square section piston rod that will prevent the spin of the lower grip. It is prepared to work in environments that range from -20°C to 80°C and is of low friction type, particularly adapted for controlled systems. Its retracting theoretical force is 2721 N, at 6 bar, while its advancing

theoretical force is 3016 N, also at 6 bar. At last, the cylinders have an integrated displacement encoder and are prepared to accommodate proximity sensors, like travel limit switches.

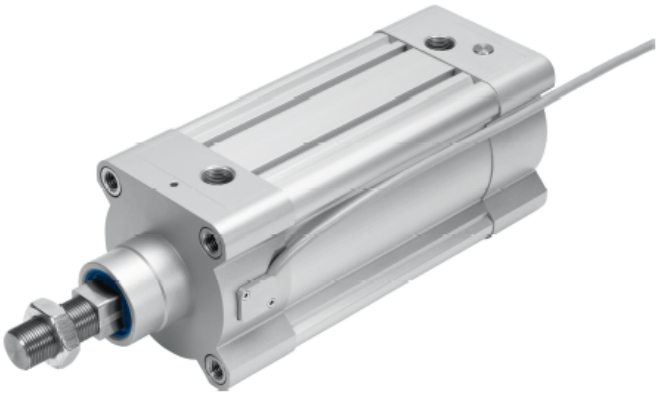

Figure 3.4: FESTO pneumatic cylinder [16]

3.2.2 Flow Control Valves

Each station is equipped with a one-way flow control valve in each chamber (two per station, six in total) controlling the exhaust of the airflow (Figure 3.5) [17]. The meter-out design helps reducing the stick slip phenomenon, improving the motion of the cylinder and effectively regulate the piston speed. Also, by restricting the airflow of the main chamber, the specimen rupture effects (impact force of the piston, spikes in pressure that may affect other stations as well) are being minimized. The flow restriction is adjusted via screw.

Figure 3.5: FESTO Flow Control Valve [17]

3.2.3 Directional Valves

The existing solution is a 5/3 in line directional valve produced by FESTO (Figure 3.6) [18]. Each station has a directional valve in its pneumatic circuit responsible for the cylinder's movement. In its closed position, or when it is disengaged, the cylinder stands still due to the valve´s closed center (minus

air leakages). When not actuated, the valve return to their closed central position by the action of mechanical springs. If the purpose is for the cylinder to move up, then the valve commutes allowing airflow into the lower chamber and connecting the upper chamber to the exhaust port. If the purpose if for the cylinder to move down, the logic is just opposite: the valve commutes allowing airflow to the upper chamber and connecting the lower chamber to the exhaust port.

The commutation of the valves is done through the use of solenoids. The solenoids operate at 24 V DC. Also, the valves are internally piloted and need, at least, 2.5 bar to be piloted.

Figure 3.6: FESTO Directional Valve [18]

3.2.4 Pressure Regulator Valves

During a creep test, being able to maintain the applied load at a constant value is of paramount importance. Therefore, a VPPX pressure regulator valve is implemented to control and regulate the pressure (and consequently the load applied) in the active chamber of the cylinder during the creep test (the upper one). The VPPX design and its schematics are shown below (Figures 3.7 and 3.8 [19].

Figure 3.7 VPPX valve [19]

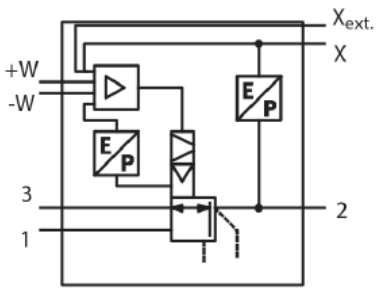

Figure 3.8 VPPX schematics [19]

The VPPX valves are designed to control pressure from 0.1 to 10 bar. The pressure regulator valves have two operation modes: the internal one and the external one. If working on the internal mode, when a setpoint value (W+) is given to the valve (via software, for instance), the integrated pressure sensor measures the pressure output at the port (X) and compares it to the setpoint value. If there is a deviation between the setpoint value and the output value, the valve regulates the output value in order to approximate its value to the setpoint one. If working on the external mode, the valve compares an external signal (Xext) to the setpoint value. If there is a deviation between the setpoint value and the external value, the valve regulates the output pressure to equalize the values of both the setpoint and the external sensor.

The VPPX connections to the electric circuit are shown in the table below (Table 3.1).

Table 3.1: VPPX's connections to the electric circuit

Pin	Assignment	Signal Voltage
1	Digital communication	-
2	+24V DC power supply	24V
3	Setpoint value W+ (analogue differential input)	0-10V
4	Setpoint value W- (analogue differential input)	0-10V
5	Digital communication	-
6	Actual value X (analogue output)	0-10V
7	0V power supply	-
8	External actual value Xext (analogue input)	0-10V

3.2.5 Air Treatment Unit

The Air treatment unit implemented is FESTO'S MSB4-AGC:C4H3:N3-WP [20]. It includes an on/off manual valve with silencer, a 5 μm filter (recommended for for the good function of the cylinders), with a plastic bowl guard, a manual condensate drain, an integrated pressure gauge and a rotary knob, that regulate the pressure value between 0.1 to 12 bar (Figure 3.9).

Figure 3.9: Air treatment unit [20]

3.3 Electric circuit

The electric circuit provides the power needed to operate the machine and establishes the connections between different systems. Some missing components were manufactured and some components had to replaced or repaired due to malfunctions present in those elements of the circuit.

The main components of the electric circuit are going to be briefly described in the forthcoming subsections. Some elements that are an active part of both electric and pneumatic circuit like the pressure regulator valves or the directional valves were already discussed previously and, for that reason, will not be a matter of discussion later in this section.

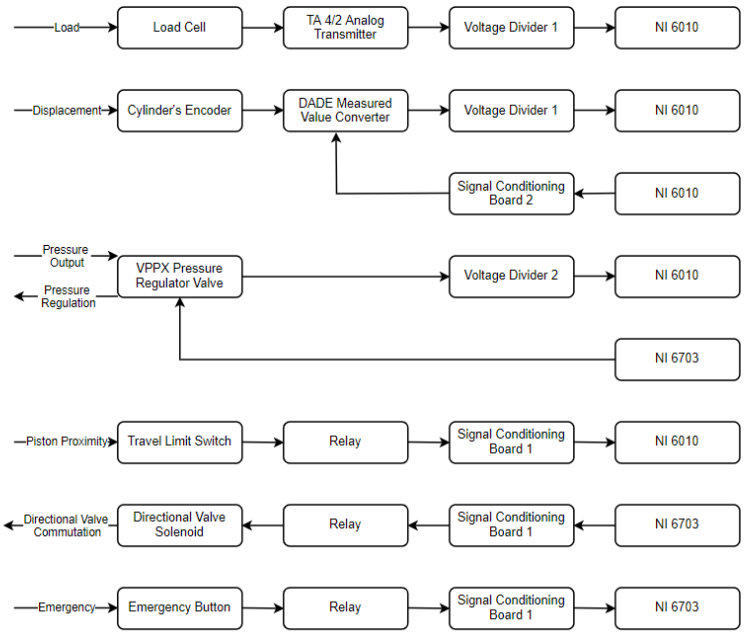

Figure 3.10: System electric communications

3.3.1 Load Cells

As previously stated, each station has a load cell implemented in its upper assembly (Figure 3.11). The load cell is responsible for measuring the load applied in the specimen during the test. More, it is the reference of control to ensure that the load applied during the test remains constant. Both the load cell and its amplifier were manufactured by AEP Transducers [21] [22]. The amplifier or transmitter feeds the load cell and receives its signals, amplifying and filtering them (Figure 3.12).

Figure 3.11: TS Load Cell [21]

Figure 3.12: TA 4/2 Analog Transmitter [22]

The load cell outputs an analog signal between a range of -10 V to 10 V (depending on the specimen being subjected to a compression load or a tension load, respectively). This corresponds to a load of -3000 N (compression) or 3000 N (tension). The load cell and the transmitter operate at 24 V DC, have a linearity error inferior to 0,02% , resolution of 0,025% and accuracy error inferior to 0,02% [21] [22].

3.3.2 Encoders

The FESTO cylinders have an integrated linear encoder. This is a relative displacement encoder which allows the user to obtain the incremental position of the cylinder. Their signal outputs are converted to DC voltage via DADE measured Value Converter (Figure 3.13) [23]. The software will be able to compare the initial position of the test with the following ones, recording the displacement of the specimen at any point in time.

Figure 3.13: FESTO DADE Measured Value Converter [23]

The encoders are powered at 24 V DC and their analog output signal ranges from 0.1 V to 9.9 V, through DADE Measured Value Converter - simply referred to as DADE from this point on. The DADE has a linearity error minor to 0.08 mm, a repetition accuracy inferior to 0.1 mm and a resolution of 0.025 [23].

The relative displacement (x), in mm, within the work stroke (assuming a 300 mm work stroke), for a measured voltage (U) is given by equation 3.1:

$$x = \frac{9.9 - U}{9.9 - 9.1} \times 300 \tag{3.1}$$

Since the integrated linear encoder is a relative displacement one, it needs to be referenced every time the power was turned off. Also, a calibration procedure is required in the first commissioning to save the cylinder's course

extension. This procedure, unlike the referencing one, is required only once, unless the DADE memory is lost or reset.

The steps of the first commissioning procedure are:

1. Switch on the operating voltage
2. Move the cylinder to the reference point (zero point of the work stroke)
3. Set the "Reference Input" for at least 0.5s
4. Reset the "Reference Input" signal. As soon as a signal is present in "Reference Output", (the response can have a delay longer than 0.1 s) the reference point is saved.
5. Move the cylinder to the end position of the work stroke and ensure the cylinder is immobilized
6. Set the "Calibration Input" for at least 0.5 s.
7. Reset the "Calibration Input" signal. As soon as a signal is present in "Ready Output", (the response can have a delay longer than 1 s) the work stroke is saved permanently.

This seven steps are only necessary in the first commissioning. After that, only the first four steps are required. Once step 4 completed, both "Reference Output" and "Ready Output" signals will be set.

The connections between the encoder and the electric circuit are displayed in table 3.2 below.

Table 3.2: DADE's connections to the eletric circuit

Pin	Assignment	Signal Voltage
1	+24 V power supply	24V
2	Measured signal (analog)	0.1 to 9.9V
3	Reference Output	0/24V
4	0V measured signal	-
5	Reference Input	0/24V
6	Calibration Output	0/24V
7	Ready Output	0/24V
8	0 V power supply	-

3.3.3 Travel Limit Switches

Each station is equipped with two FESTO SMT magneto-resistive proximity sensors (six in total), Figure 3.14 [24]. These sensors are compatible with the cylinders. The operating voltage of the sensors is 24 V and they switch their normally open contact when sensing the piston rod. When activated, the sensors trigger a respective relay, that prohibits the directional valves to allow airflow to the relevant chamber. For example, if the cylinder is moving down and reaches the lower travel limit switch, trigger the relay that blocks the directional valve to allow airflow into the upper chamber. The two sensors in each station delimit the cylinder's travel.

Figure 3.14: FESTO SMT proximity sensor [24]

3.3.4 Data Acquisition System

The Data Acquisition System is the bridge that connects the computer and software to the machine and its hardware. By using a computer to control the machine and record the data, it is necessary to acquire and generate signals (analog inputs and outputs and digital inputs and outputs).

Therefore, the PC must be equipped in order to interact with the machine´s hardware and interpret their signals. Since a lot of signals must be acquired or generated, two Data Acquisition Boards from National Instruments [25], the company that develops LabVIEW, are installed in the computer and connected to the electric circuit. The specific connections through pins and channels will be brought up later in this dissertation.

The first board is NI-PCI-6010 (Figure 3.15). This board operates in a range between -5V and 5V for both input and output analog signals. The digital signals of this device are 5 V ones. It contains sixteen analog input channels (AI), two analog output channels (AO), six digital input (DI) channels and four digital output (DO) channels [26].

Figure 3.15: NI-PCI-6010 DAQ Board [26]

The other board is NI-PCI-6703 (Figure 3.16). This board does not possess any analog input channel. However, it compensates that fact and the lack of output analog channels present in the NI-PCI-6010 by having sixteen analog output channels. Also, it features eight digital channels - can function as both digital inputs or digital outputs. This board's analog output signal ranges from 0 V to 10 V. As for the digital signals, identical to the NI-PCI-6010, this boards' ones are also 5 V[27].

Figure 3.16: NI-PCI-6703 DAQ Board [27]

The standard signals of the electric circuit are of 24 V. Also, the analog outputs of the load cell and the cylinder's encoders as well as the analog inputs and outputs of the VPPX pressure regulator valve can vary between 0.1 V and 9.9 V [19]. Since, both of he boards, whether the signal is digital or analog, function with signals no greater than 5 V, all of these signals from the hardware require conditioning before arriving to the DAQ boards.

3.3.5 Signal Conditioning System

The signal conditioning system can be divided in two categories: signal conditioning for analog signals and signal conditioning for the digital ones.

The analog signals that require signal conditioning are the ones from the load cells, the DADE's encoders and the VPPX ones.

The load cells transmitter output ranges from -10 V and 10 V. One could argue that since the creep test is a tensile one, there is no need for measuring the compression value, this is, the negative range of the load cell transmitter, and the load cell output value could be acquired by the NI-PC-6703, whose analog signals range from 0 to 10 V. However, that board does not have any analog input channel and therefore cannot accommodate the load cell transmitter signal.

The encoders output signal ranges from 0 V 10 V. Pina [4], in his dissertation, has demonstrated that converting that range to 0 V to 5V provides none loss of resolution.

Silva [5], in his thesis, evidenced that halving the range of the VPPX, 0 to 10 V, in an identical manner to the encoders, also does not influence the resolution of the pressure regulator valves.

For this output signals to become compatible with the data acquisition board ones, two voltage divider systems were implemented. Using identical resistors, the system can halve the signals received from these three transducers. Voltage divider board 1 halves the voltage of output analog signals from the load cells and the DADE, while voltage divider board 2 halves the voltage of the output analog signals of the VPPX (Figures 3.17 and 3.18).

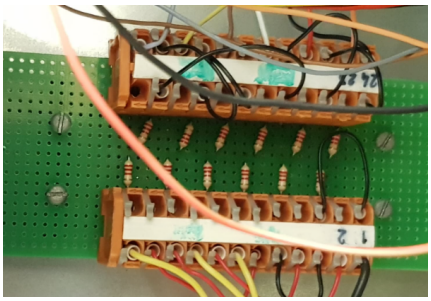

Figure 3.17: Voltage Divider 1

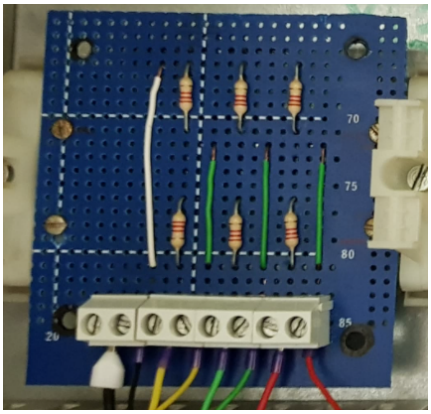

Figure 3.18: Voltage Divider 2

As for the digital signals, they need to be converted from 24 V to 5 V. Also the output of the data acquisition boards has to be converted in the opposite fashion: from 5 V to 24 V. In order to accomplish this, two signal conditioning boards were implemented.

The first one has eight channels for the computer outputs, called PC OUT, and eight channels for the computer inputs, named PC IN (Figure 3.19). The PC OUT conditions the signal directed to the actuation of the directional valves (six channels) and the emergency relay. When these signals are set to 5 V, an output of 24 V is given to the electric circuit. The PC IN channels condition the signal of the travel limit switches (six channels) and the Emergency button arriving to the computer. When presented with a 24 V signal, an output of 5V is given to the DAQ boards.

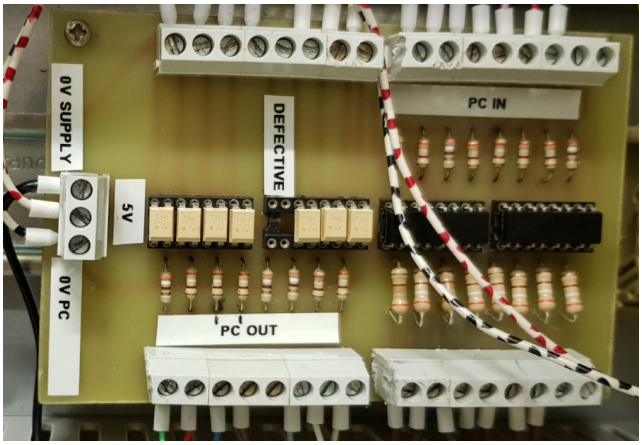

Figure 3.19: Signal Conditioning Board 1

The second one has twelve channels. Four of them are for the PC OUT channels and eight for the PC in channels (Figure 3.20). This digital signal conditioning board only connects with the NI-PCI-6010, once all the remain digital signals that required conditioning are going to be acquired or generated by that board. Those signals are exclusively related to the encoders and their referencing and calibration system. On the PC OUT channels are conditioned the "Reference Input" signals (three) and the PC IN channels are connected the "Reference Output" and "Ready Output" channels (six). Given that the calibration process only is required at first commissioning it was not included in the electric circuit. When the first commissioning procedure was attempted, the "Calibration Input" of each encoder was simply added to the vacant PC OUT channel (one at a time) and then disconnected once it was no longer needed.

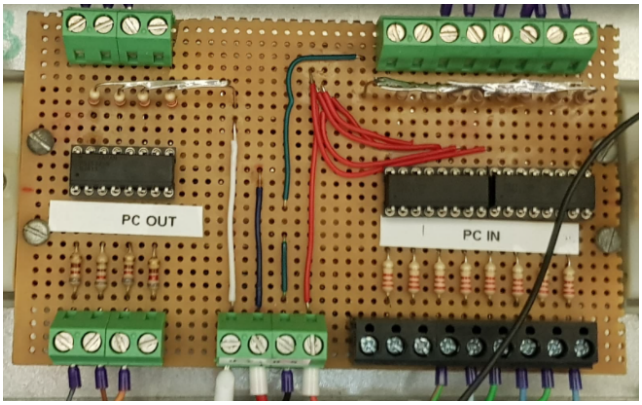

Figure 3.20: Signal Conditioning Board 2

The signal conditioning board 2 had to be manufactured and implemented in the electric circuit, according to the schematics previously designed by Silva. Also, the signal conditioning board 1 had to be fixed - some resistors had to be swapped for ones with more potency and some lanes of the board had to be weld one more time.

After the implementation of both fully functional boards on the circuit, the electric cabinet now accommodates all the elements and connections needed to provide the power and transport and condition the signals between the computer and hardware.

As stated previously, in the introduction of this chapter, the main design of the machine and its circuits were done in previous dissertations, with exception of a conditioning board. The pneumatic circuit was rearranged in some stations and some components of the electric circuit were repaired or replaced. Although, the main work described in this chapter is prior to this thesis, it is important to point out the structure of the pneumatic and electric circuits as well as their components to better understand how they interact with the software in the next chapters.

Chapter 4
Software

This chapter will address the software implemented and the system behaviour behind the machine.

The machine is a three-station creep machine for adhesive joints testing. It is designed to perform independent tests in terms of load applied and time elapsed that can be conducted simultaneously. The interface and functional code of Station 3 was already implemented by Silva [5]. Since the interface and its transitions were working properly, only some details were changed. However, the code itself regarding the functioning of the stations as well as the signals acquisition suffered changes that allowed the machine to function as it was designed to, enhance its performance and produce reliable results. The overall functioning of the machine is described in this chapter, while pointing out some of the changes implemented. In Chapter 5, other functional changes to the machine's program will be described.

4.1 LabVIEW

Software LabVIEW (Laboratory Virtual Instruments Engineering Workbench) was adopted to control the creep testing machine. LabVIEW is a visual programming language developed by National Instruments.

Labview is a graphical programming language that uses icons (elements) instead of the conventional text based languages in order to create applications [28]. In contrast with those languages, where instructions determine the execution of the program, LabVIEW determines the form of execution through the data flow [29].

The machine could be controlled using other softwares rather than LabVIEW, such as MatLab or even C or Python. LabVIEW was chosen because the data acquisition boards are from National Instruments and LabVIEW has built-in VIs that facilitate the programming involving those boards. Also, the graphical environment is more friendly in case some alterations or improvements need to be implemented to enhance the machine capabilities. Lastly, this software is being used in other machines in the AJPU lab, so the future users of this machine are already acquainted with this software.

LabVIEW's interface is divided in two panels: the front panel and the

block diagram panel. The front panel, or user interface, is the window through which the user interacts with the program. It allows interaction with the VI, inputting controls and also seeing results [30]. The input data to the executing program is fed through the front panel and the output can also be viewed on the front panel, thus making it indispensable [29]. The block diagram contains the graphic code that determines the functionality of the VI. The block diagram window holds the graphical source code of a LabVIEW's block diagram, which corresponds to the lines of text found in a more conventional language like C or BASIC – it is the actual executable code. The block diagram can be constructed with the basic blocks such as: terminals, nodes, and wires [31] [30].

4.2 State Machines

The state machine is a tool that has been used by programmers in multiple software platforms because it is a fast, easy way to develop software. A state machine is a very flexible tool that can be used by LabVIEW programmers in order to facilitate the maintenance, register and reuse of the code [32].

By definition, a Finite State Machine is a model of computation based on a hypothetical machine made of one or more states. Only one single state of this machine can be active at a time. This means the machine has to transition from one state to another in order to perform different actions. The state will change based on inputs, providing the resulting output for the implemented changes [33].

State machines revolve around three concepts: state, event and action. The state is the position, stage or status that the program is currently at and is waiting for an external object (user inputs, timers, counters, hardware response) or running some internal calculations. An event is an occurrence in time that has specific meaning to the code running in the state machine, for example clicking a button. Actions are the way the program reacts to the event. The state machine depending on the event determines what action needs to take place by knowing the current state and the triggering event [34].

The architecture of a state machine in LabVIEW is quite simple: a case structure contained inside a while loop. The while loop allows the program to run continuously until the conditional operator is set to "False". The case structure itself contains the main code of the program: each case contains the code to be executed for each state. The case selected to run is usually determined by the former iteration of the while loop as the necessary information and data for the state transition is carried via shift register. One exception is the first or default state that is always the initial state of a certain state machine[32] [34].

4.3 General Architecture

The system was designed so that the three stations are able to perform independently and simultaneously, both executing the program and recording the data. Such responsibility relies in a structural concept applied to the program where the code that executes the different and, mostly, sequential tasks is inserted (Figure 4.1).

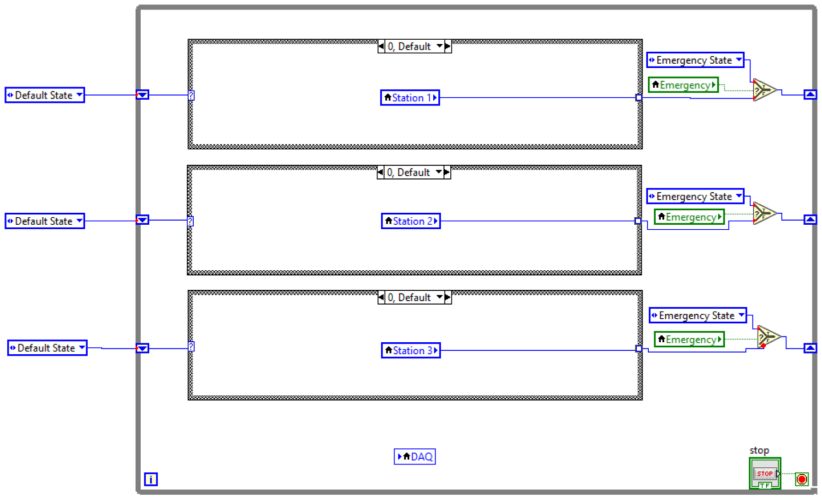

Figure 4.1: General structure of the program

The program is built as a state machine. As explained above, this program, like every state machine developed in LabVIEW, is composed by a while loop, a case structure, shift registers and transition code.

The while loop shelters all the code, - through the case structures - except the indicator of the default state to force the system to always start the program through that particular state, the DAQ system (outside of the case structure) and allows the program to run continuously executing the various states. There are three case structures inside the while loop - one for each station. The different cases of the same case structure correspond to the different states of our state machine and to the different menus of the interface. The shift register feeds the condition to run the state as an input and the output condition of that same state is fed via shift register to the next iteration of the loop as an a input condition. Finally, we have the transition code. The transition code, as the name suggests, is the part of the code responsible for the change of status of the program, for the transition between states. Such transition occurs when certain desirable conditions are met. For example, in Figure 4.1 outside of the case structure we have a select block. If the emergency relay is activated, then in the next loop the system advances to the "Emergency" state. Else, in the following loop the input is fed with the output of the case structure. Also, there is a stop button that allows the user to end the machine program at any point.

That "indicator" outside of the while loop is actually an enumerated type. The enumerated constant is the case selector, always starting with the default case. The "enum" when connected to the case selector, alters the latter's numeric index to the enumerated text. This alternative has some benefits over using an integer or a string like readability and maintenance.

As previously stated, each case structure contains the code for each station. Although the station behaviour is the same, the code should be executed independently and simultaneously for each station.

Each station has eight states that correspond to eight interface screens the user can interact with. Also, because some states need a sequential order in their process, those states are divided in a number of substates. Seven out of the eight states are connected through transitions. The exception is the "Emergency state" that, having the condition brought above outside of the case structure, can override any of the other states. Otherwise, the program runs without transitioning to the emergency state. The states and the logic behind their transitions are displayed in the graphic below (Figure 4.2).

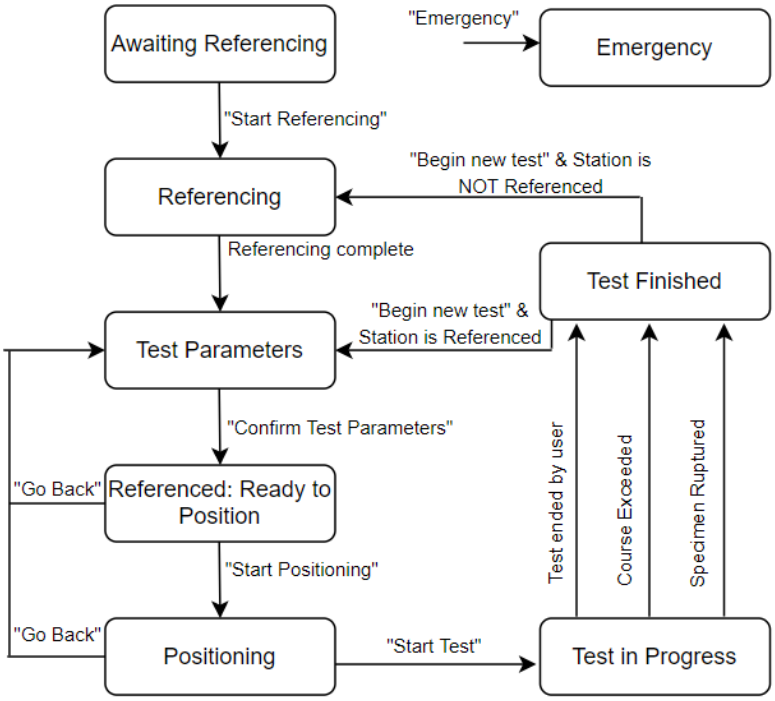

Figure 4.2: General station structure

4.4 DAQ - Data acquisition

This section addresses an important feature of the machine as a whole: the connection between hardware and software. This topic is not anything new. Said connections were already analyzed in chapter 3, mentioning the signal conditioning boards and the NI DAQ boards. However, software was,

at that time, omitted. In this section it will be provided a detailed explanation of how data is manipulated by LabVIEW and how the virtual connections are tangled with the physical, electrical ones.

Below, in Tables 4.1 and 4.2 are registered the used channels of DAQ boards NI6010 and NI 6703, respectively, and associated with the respective hardware and signal.

Table 4.1: NI 6010

Channel	Pin	System	Description
		DADE 1	0 V Measured Signal
AI GND	25	DADE 2	0 V Measured Signal
		DADE 3	0 V Measured Signal
AI 0	1	DADE 1	Measured Signal (Analogue)
AI 1	21	DADE 2	Measured Signal (Analogue)
AI 2	22	DADE 3	Measured Signal (Analogue)
AI 3	5	VPPX1	Analogue Output X
AI 4	6	VPPX2	Analogue Output X
AI 5	26	VPPX3	Analogue Output X
AI 7	28	FDC1	Cyl. 1 : Upper Prox. Switch
AI 8	20	FDC2	Cyl. 1 : Lower Prox. Switch
AI 9 (V)	2	FDC3	Cyl. 2 : Upper Prox. Switch
AI 10	4	FDC4	Cyl. 2 : Lower Prox. Switch
AI 11	23	FDC5	Cyl. 3 : Upper Prox. Switch
AI 12	25	FDC6	Cyl. 3 : Lower Prox. Switch
AI 13	7	LCell1	Load Cell 1: Transmitter
AI 14	9	LCell2	Load Cell 2: Transmitter
AI 15	10	LCell3	Load Cell 3: Transmitter
PFI 0/P0.0	13	DADE 1	Reference Output
PFI 1/P0.1	32	DADE 1	Ready Output
PFI 2/P0.2	33	DADE 2	Reference Output
PFI 3/P0.3	15	DADE 2	Ready Output
PFI 4/P0.4	34	DADE 3	Reference Output
PFI 5/P0.5	35	DADE 3	Ready Output
PFI 6/P1.0	17	DADE 1	Reference Input
PFI 7/P1.1	36	DADE 2	Reference Input
PFI 8/P1.2	37	DADE 3	Reference Input
PFI 9/P1.3	19	PC EMER	Emerg. Relay (PC)

Table 4.2: NI 6703

Channel	Pin	System	Description
AO 0 (V)	34	VPPX1	Analogue Input W+
AO GND	68	VPPX1	Analogue Input W-
AO 1 (V)	66	VPPX1	Analogue Input X_{ext}
AO 2 (V)	31	VPPX2	Analogue Input W+
AO GND 2	65	VPPX2	Analogue Input W-
AO 3 (V)	63	VPPX2	Analogue Input X_{ext}
AO 4 (V)	28	VPPX3	Analogue Input W+
AO GND 4	62	VPPX3	Analogue Input W-
AO 5 (V)	34	VPPX3	Analogue Input X_{ext}
P0.0	2	EMERG	Emergency button
P0.1	3	DV 1 UP	Direction Valve 1: UP
P0.2	4	DV 1 DOWN	Direction Valve 1: DOWN
P0.3	5	DV 2 UP	Direction Valve 2: UP
P0.4	6	DV 2 DOWN	Direction Valve 2: DOWN
P0.5	7	DV 3 UP	Direction Valve 3: UP
P0.6	8	DV 3 DOWN	Direction Valve 3: DOWN
D GND	36	-	Signal Conditioning Boards GND
+5 V	1	-	Signal Conditioning Boards +5 V

Using these tables, the system was programmed by associating the variables in the software with the channels of the DAQ boards. Within the myriad of tool kits, add-on VIs, made available by LabVIEW, there is one called DAQ assistant.

The DAQ assistant is the tool that allows the software to acquire or generate the signals [25]. DAQ assistants can only signal inputs or outputs, never both. Also, digital and analog inputs and outputs require different DAQ assistants. That information is fed to the DAQ assistant when creating and configuring the DAQ block.

After that, it can be configured in terms of the voltage range of those signals, the acquisition mode, the terminal configuration, the triggering, etc. (Figure 4.4).

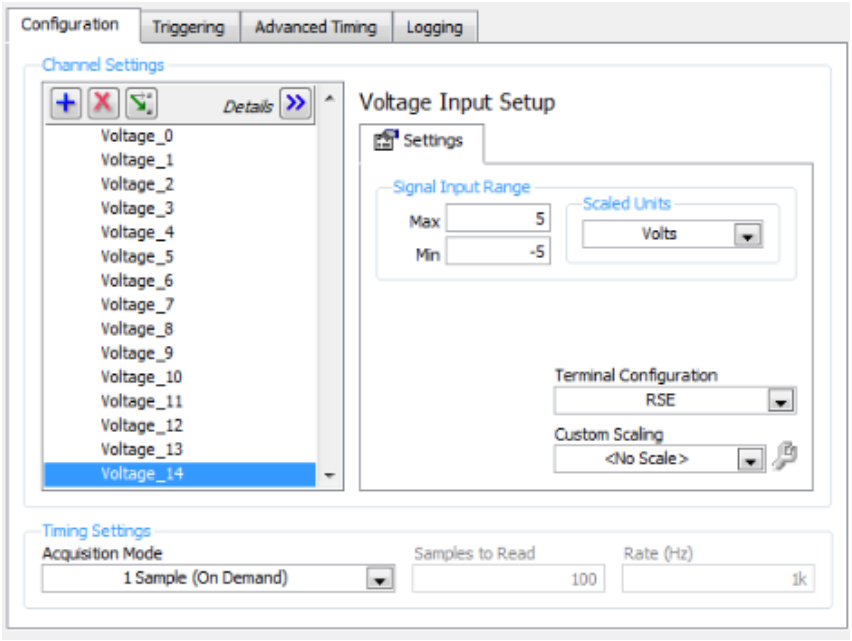

Figure 4.3: DAQ assistant configuration

Based on the tables above, that organize the connections between the hardware and the computer, the software variables were assigned to the corresponding channel. The software channels and connections are displayed in Figure 4.4 below. For instance, "Voltage0" is connected to the "AI 0" channel of the NI 6010 board, meaning "Voltage0" refers to the analog output of the DADE measurement signal.

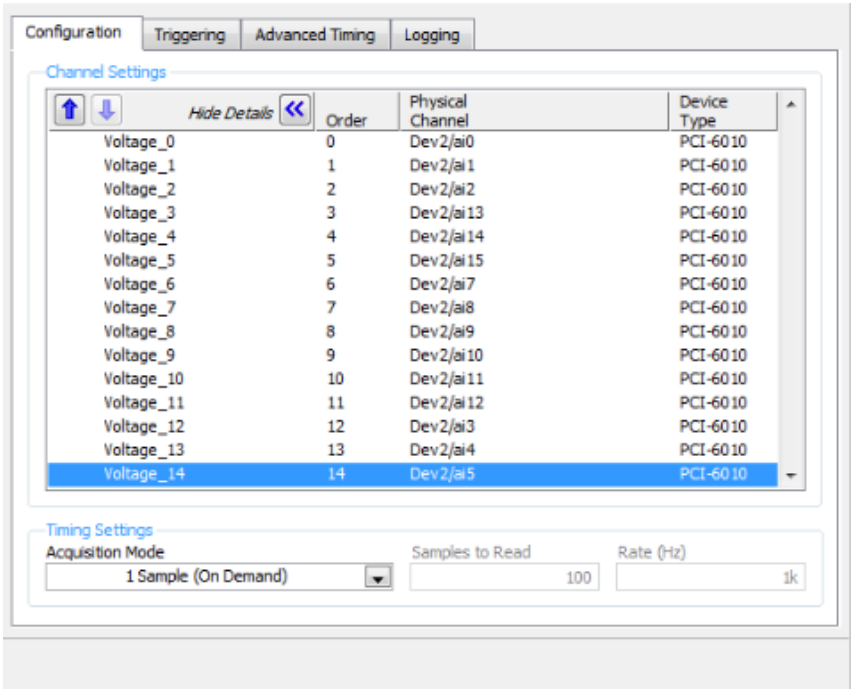

Figure 4.4: DAQ assistant used channels

In Figure 4.5, only the station 1 DAQ established connections are displayed. Nevertheless, the same logic was applied to the other two stations. For instance, the "DAQ Assist AI" block which has 5 connections regarding Station 1, has actually 15 connections, being the other 10 (corresponding to Stations 2 and 3) added and connected to the corresponding channels previously exposed in Tables 4.1 and 4.2.

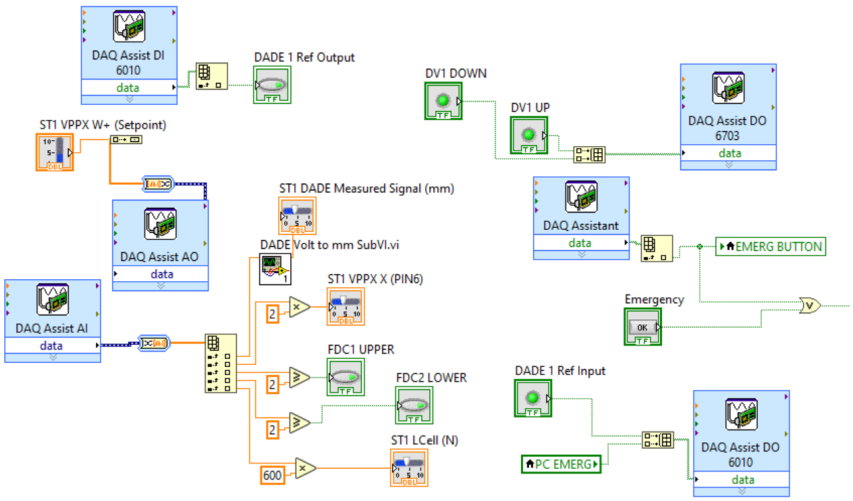

Figure 4.5: DAQ assistant blocks and connections

Regarding NI 6010 DAQ board, the system requires three assistants (AI, DI, DO). The digital input DAQ assistant is responsible for receiving the "Reference Output" signal. The green lines refer to Boolean variables, therefore they are used by the software to link discrete signals such as the digital ones. The digital output DAQ assistant carries out the signals from the also discrete signals: "Reference Input" and the "PC EMERG" local variable, that will be explored in the forthcoming section. The only difference in establishing these connections, besides that the operations are inverse, is the gathering and organizing the data. If dealing with inputs, then a Index Array must be used (even if there is only one signal being acquired) to sort out the data, to separate the different voltage sources and to separate the different elements. If dealing with outputs, then a Build Array must be used to combine the different local variables before sending the information to the DAQ assistant block.

Another DAQ assistant handles the analog inputs connected to this board. The block output contains both voltage and time information (blue line). To strip the time information of this Dynamic Data, a Dynamic Data Converter is attached to the output of the block. After, a Index Array is used to separate the voltage from the different elements connected to the DAQ assistant block. From the five variables the computer is reading, DADE measuring system is the first one. The analog voltage is converted into displacement, using the theoretical calculation provided by Festo and described previously. For that effect, a sub-VI is used. A sub-VI is a sub-routine, called in the main routine: a program within a bigger program. This particular sub-VI is just a

equation that allows the conversion of the analog voltage into the displacement of the cylinder. The VPPX output signal is being multiplied by two due to the different analog ranges between the two boards. The VPPX output signal should be approximately equal (in theory, numerically equal) to the VPPX setpoint signal. However, since these signals are being acquired and generated in different DAQ boards and the NI 6010 has an analog range between -5V and 5V and NI 6703 has an analog range between 0 and 10V, there is the need to double the signal of the VPPX analog output. The next two variables are the travel limit switches. As there was a lack of digital input channels, the travel limit switches were connected to analog inputs. In order to correct that situation, a threshold was used for comparison. If the output signal is bigger than 2 V, then the travel limit switches are activated. At last, there is the output signal from the load cell. Once the load cells measure from -3 kN to 3 kN and its output voltage ranges from -5V to 5V, the immediate solution was to apply a gain of 600 to that signal, in order to convert the voltage to the load applied in the load cells.

As for the NI 6703 DAQ board, the procedure is very similar (only the variables change) and, for that reason, the analysis of this board connections can be omitted.

4.5 GUI and Code

In the following subsections, a detailed analysis of the functional behaviour of every state (and, in some cases, substates) will be provided. Said analysis will focus on both the Graphical User Interface (GUI) and the source code on the block diagram.

Since all stations share the same behaviour, the following subsections will only address station 1, providing a more clear, succinct, simple and less redundant detailed explanation of the system behaviour.

4.5.1 State: Awaiting Referencing

This is the first and simpler state of the system, also the default one meaning that every time the machine is turned on, it opens up this menu. In the first loop and independently of the values previously stored, the program ensures that the "Awaiting Reference" state is always and without fault the starting point of the sequential structure.

As said above, the current state is extraordinarily simple, as shown in Figure 4.6. It is only waiting for the order, by pressing the button, to transition to the next state ("Referencing"): the encoders need referencing prior to the execution of the tests whenever they are turned on.

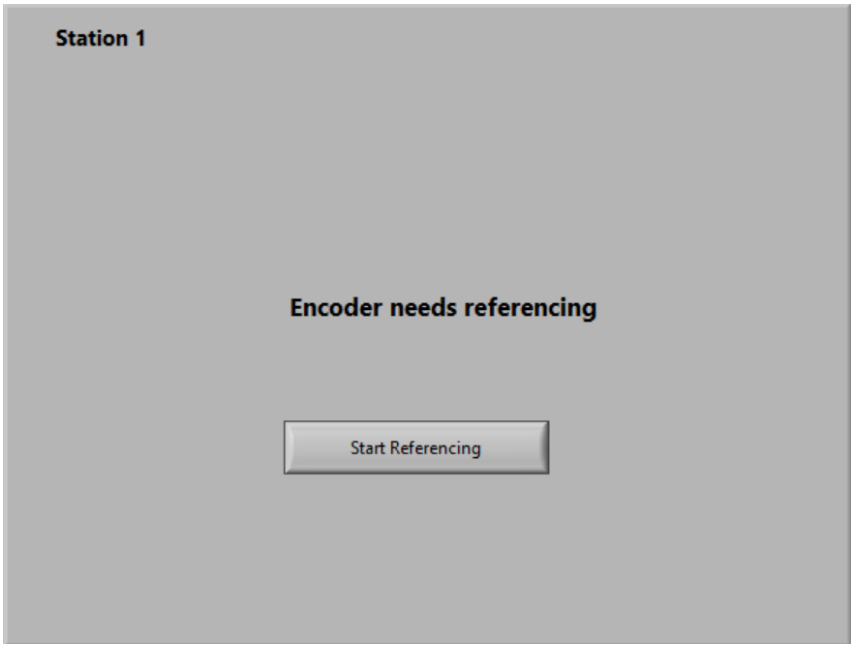

Figure 4.6: Awaiting Reference menu - GUI

However, this first state is used to ensure that some variables (whether auxiliary or physical) are reset, as shown in the Figure 4.7.

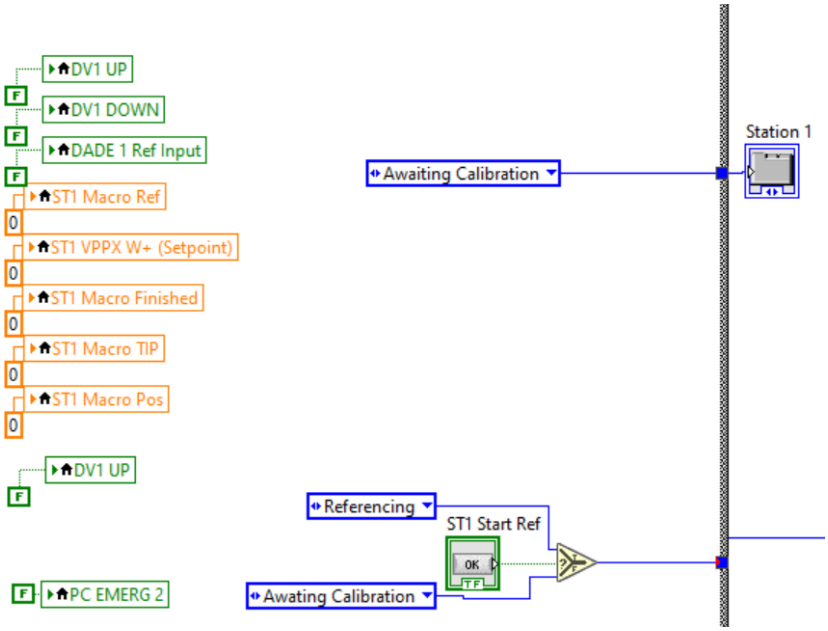

Figure 4.7: Awaiting Reference block diagram

In that same figure, there is an "enum" variable that displays "Awaiting Reference" connected to a Station 1 indicator outside of the case structure . This added detail allows the program to keep track of the menu of the interface that it is being displayed and improves the readability, the organization and

the maintenance, case some alterations are needed in the future, of the code that runs behind the interface.

4.5.2 State: Referencing

As exposed in the previous subsection, the encoder needs referencing when being turned on. The reason behind this is bounded to the fact that the encoder is relative which means it reads incremental values. Since the encoder is directly responsible for both measuring the claw distance during the positioning of the machine that allows the placing of the specimen and measuring the deformation of the specimen during the tests, this procedure that precedes the test itself, is mandatory for the good function of the system. Also, this state requires the user to confirm that the station is clear before any action or cylinder movement take place (Figure 4.8).

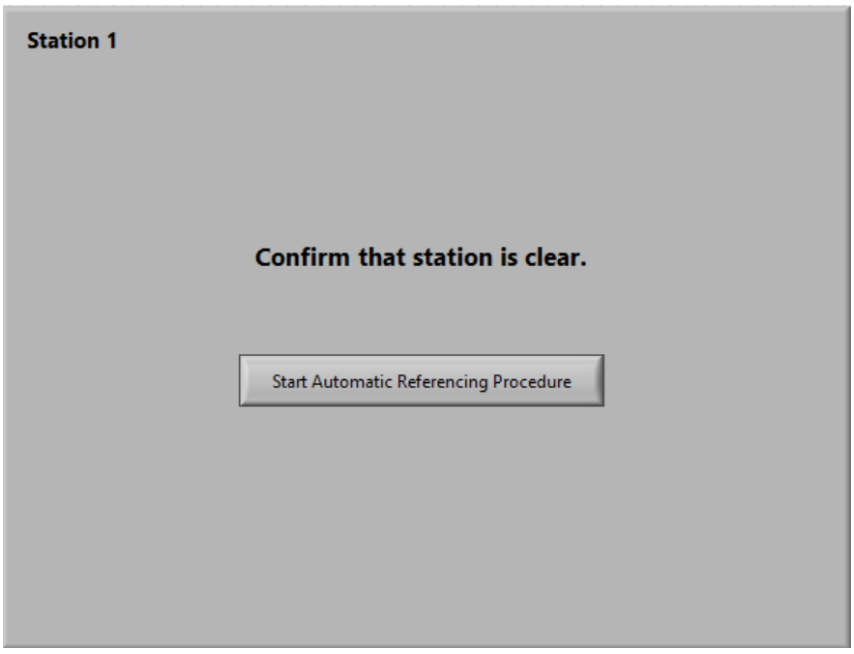

Figure 4.8: Reference GUI menu

The “Referencing state” is composed by four substates. Such is achieved by creating a case structure inside our main case structure and by defining a auxiliary variable – “Macro Ref”- that is responsible for the transition between substates and for showcasing the substate that the program is currently running.

In the first state – substate 0 - it is ensured that the directional valve is closed (by attributing the value “false” to both DVUP and DVDOWN). The system is brought forward to the next state by pressing the button in the interface that confirms that the station is clear. Inside the substate there is another case structure merely to allow the transition from substate to substate within the same state and therefore the same menu of the interface.

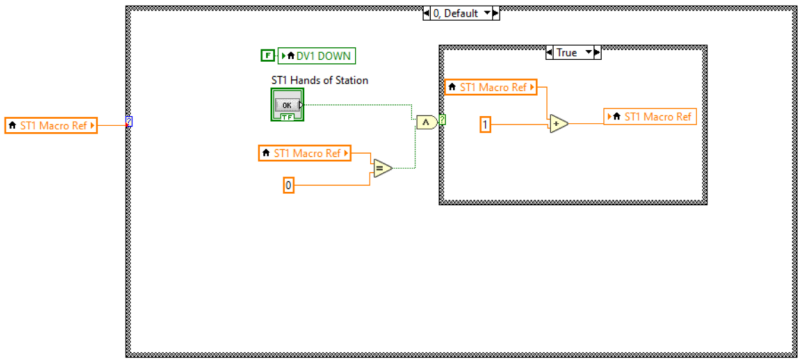

Figure 4.9: Block Diagram of substate 0

In substate 1, the VPPX (pressure regulator valve) pressure is set to 3 bar and the solenoid of the directional valve is actuated to allow airflow into the upper chamber of the cylinder, making it descend (if it isn't already on its lower position).

When the lower travel switch is activated, the program enters substate 2, the VPPX is once again set to 0 bar and the directional valve is disengaged and the DADE Reference Input is set to "True". After 0.5 s the program transits to the last sub state where the DADE Reference Input is reset.

In substate 3, if the value of DADE Output Reference is "True" then the machine changes to the "Test Parameters" state and the referencing procedure was successful. Otherwise, if after two seconds there was no high signal of DADE Reference Output, it means the procedure was not successful. The machine goes back to stage 0 and awaits confirmation that the station is clear.

The structure of the current state is displayed in the schematics below (Figure 4.10).

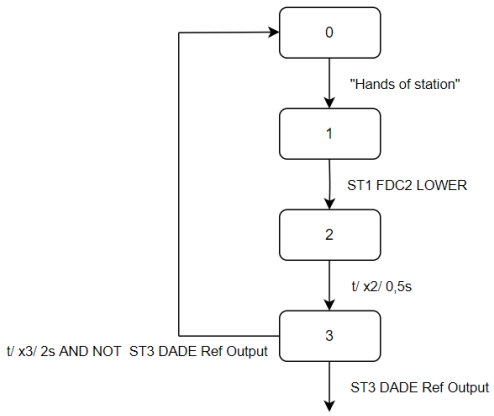

Figure 4.10: Structure schematics of "Referencing" state

4.5.3 State: Test Parameters

This state has a very simple structure. Its interface is composed by three input boxes that set the test parameters: desired load, sample rate and specimen weight (Figure 4.11). The first one allows the user to choose the constant applied to the specimen, albeit the values available to the user are comprehended between 100 N and 2800 N (limits imposed by the hardware system in which the machine can perform creep tests) in minimal increments of 5 N. The second one defines the number of samples that are recorded each minute and only requires the user inputs a positive number (multiples of 5). The third one allows, if the user elects to, the adding of the weight of the specimen that will later influence the calculations regarding the load applied. The user can input any integer value between 0 and 1000 g, being zero the default value case the user finds the weight of the specimen can be despised.

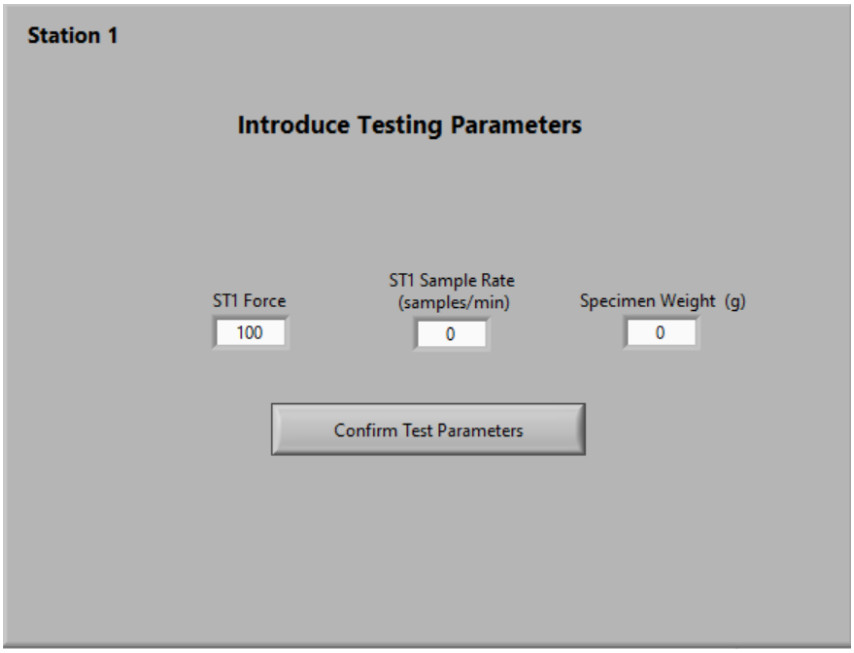

Figure 4.11: Test parameters GUI menu

Whenever this conditions aren't met, the program will coerce the data entry to follow its specifications. For instance, if the user inputs a load of 3000 N (only half of the limit load measured by the load cells but over the limit of the imposed by the software - 2800 N), the program will coerce the value back to 2800 N - maximum load allowed. If when choosing the sample rates per minute, the user doesn't introduce a multiple of 5, the program will coerce the input value to the nearest multiple of 5 (if the user inputs "7", it will coerce the value down to 5. If he inputs "8", it will coerce the value up to 10).

After defining both test variables, the system awaits that the user presses "Confirm Test Parameters" and the interface displays the next state: "Referenced: Ready to position".

4.5.4 State: Referenced: Ready to Position

This state is displayed in the interface after the user had confirmed the test parameters in the previous state. Its architecture is quite simple: the load,sample rate and specimen weight inputs are shown and the user is present with two options - advancing to the positioning of the cylinder in order to place the specimen or go back to alter the test parameters (Figure 4.12). This stage works as a safety net in case of an introduction and confirmation of incorrect, undesirable values in the "Test Parameters" state.

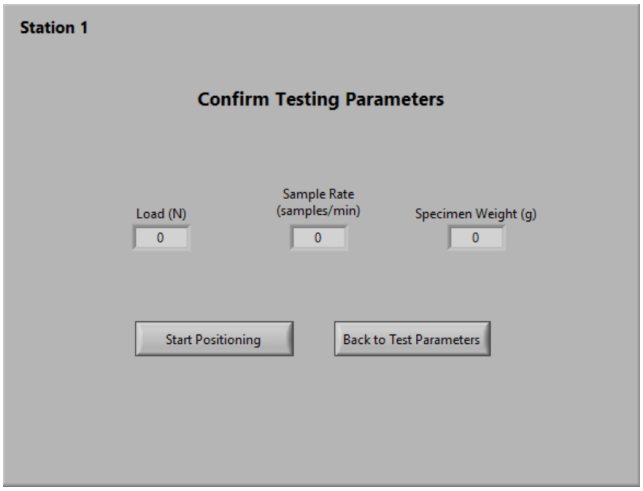

Figure 4.12: "Referenced: Ready to position" GUI menu

Besides the buttons presented in the interface, the block diagram contains two property nodes regarding those buttons, as shown in Fig. 4.13. Their function is ensuring that when the machine enters this state, those buttons are always reset ("unclicked"). A good example of the need for this status reset allowed by the property nodes is when the user decides to go back to the test parameters. Once returning to the current state, the "Go back" button will appear unpressed, instead of appearing pressed due to the nonexistence of a method to reset the buttons' status. This property node implemented detail is repeated in further states of the program, but due to its simplicity and because the exact same logic is applied, it will not be evidenced again.

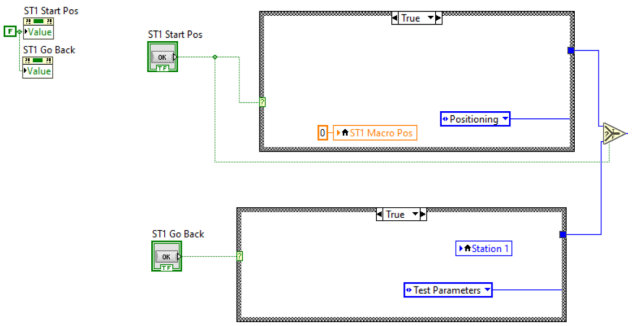

Figure 4.13: "Referenced: Ready to Pos" Block Diagram

4.5.5 State: Positioning

The "Positioning" state, containing several substates, is programmed to ensure the positioning of the lower claw at the desired height to allow the user to place the specimen that will be subjected to the creep test, while allowing to "zero" some variables (displacement and load cell).

In the current state, there is a variable that accounts for the different stages of this submachine. Working in similar form to "Macro Ref" in the "Referencing" state, the local auxiliary variable "Macro Pos" feeds the case structure of this submachine the information that allows the transitions between stages, according to the logic presented in Figure 4.14 .

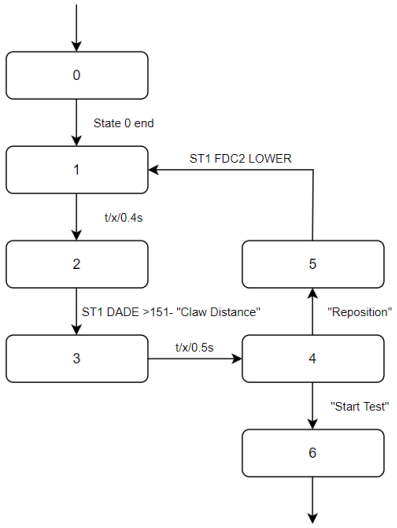

Figure 4.14: "Positioning" state schematics

Since this is the biggest and most complex state of the program, where a lot of values, measures and equations come from experimental processes and approximations, it will be approached in a more segmented way (state by state) in order to better understand the behaviour of the system.

4.5.5.1 Positioning: State 0

The directional valve is disengaged (set to the closed state) and the VPPX pressure regulator valve is set to 0 bar. The cylinder remains in the lowest course position, once it has not been moved since the descent provoked in the "Referencing" state. The function of this state is essentially to make sure the variables behind the hardware behaviour above exposed are reset.

Regarding the interface, two buttons are disable and grayed out: the "Go back" one and the "Start test" one. Besides those buttons, other buttons present in the GUI ("Reposition", "Zero Load Cell", "Zero Position" and "Claw distance") will be addressed in further states of the "Positioning" process. There is also an indicator on the top of the panel coloured in dark green,

informing the user to wait.

4.5.5.2 Positioning: State 1

In state 1 of the "Positioning" machine, the directional valve is activated to allow airflow to the upper chamber of the cylinder. Also, the VPPX is opened to the maximum, meaning that the airflow entering the upper chamber will be pressurized at 6 bar (limit imposed by the Air Treatment Unit). After 400 ms the station moves on to state 2.

4.5.5.3 Positioning: State 2

The directional valve is set to allow airflow to the lower chamber in order to the cylinder to ascend. Also, the VPPX valve setpoint is once again set to 0 bar. However, since the flow control valves are heavily restricting the airflow (they are pretty much closed) of the upper chamber, a counter-pressure is established (once in the previous state the upper chamber was pressurized), preventing the cylinder to move up too fast, even if the lower chamber is at maximum pressure - 6 bar.

Once the DADE measured signal, in milimeters, is greater than 151 minus the desired claw distance, the station advances to state 3. The claw distance can be set in the interface, choosing any integer value between 15 and 200 mm.

4.5.5.4 Positioning: State 3

The VPPX valve is once again open to the maximum and the directional valve actuated allowing airflow to the upper chamber, recreating a counter-pressure opposing the upwards movement of the cylinder. After 500 ms, the machine enters the next state.

4.5.5.5 Positioning: State 4

The directional valve returns to its central position and blocks airflow from and to the cylinder's chambers. By being disengaged and because both chambers have approximately the same pressure but the upper chamber has a smaller area due to the piston, the resulting force provokes the cylinder to move upwards until the forces become equalized. The resulting force must be null when the distance between the upper and lower assembly is equal to the "Claw Distance" the user chose and wrote in the screen. Since the trend is that the cylinder maintains its ascending movement surpassing the intended displacement, a condition was imposed. If the cylinder reaches the upper travel limit sensor or the DADE measured value is greater than 254 mm (the distance between the grips when the cylinder's piston is at it lowest point) minus the desired claw distance for the specimen placement, the directional valve allows airflow to the upper chamber, forcing the cylinder to descend until the DADE measured value is equal to 254 mm minus the desired claw

distance. Sometimes, it takes the cylinder a while to find balance, moving up and down in low increments around the desired distance until the forces equalize, and the cylinder stops with good precision regarding the intended position. 20 s after reaching 200 mm of the course, the station has reached an equilibrium of forces at the desired position and stopped moving or it is ever so slightly finding a balance around the claw distance input. At that point, the interface, that so far, displayed a LED in dark green commanding the user to wait (Figure 4.15), now displays a green LED allowing the placement of the specimen (Figure 4.16). Also, the "Start Test" button and the "Go Back" button are now enabled. By clicking on the "Go Back" button the user return to the "Test Parameters menu" and by clicking the "Start Test" one the user elects to start the creep test. The remaining buttons on the interface ("Zero Load Cell", "Zero Position" and "Reposition") can be clicked at any time during the Positioning state. The "Reposition" button allows the user to change the intended claw distance, by making the cylinder descend until the lower travel switch and start the procedure over again. The other two buttons are very similar to one another: the user can "zero" the load cells and the position at any time in the interface. Finally, there is a file path in the interface that pops-up when the machine enters this substate and forces the user to choose or create a file to save the data of the ensuing creep test.

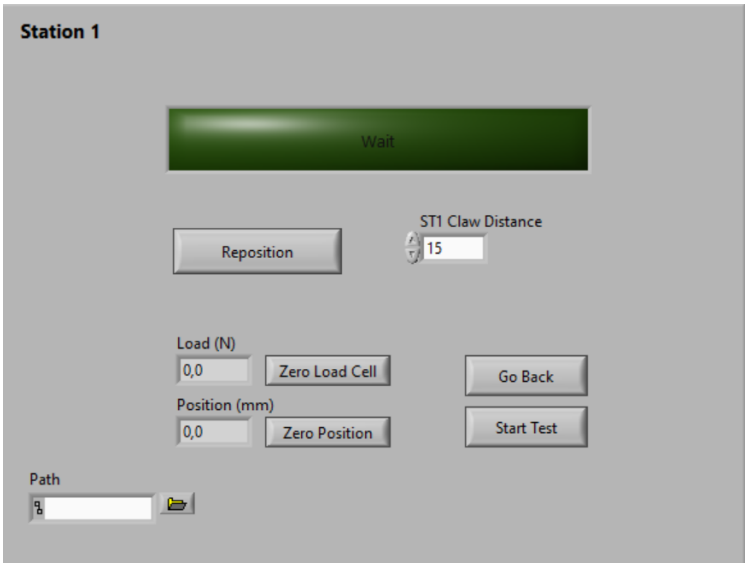

Figure 4.15: Positioning GUI menu- awaiting

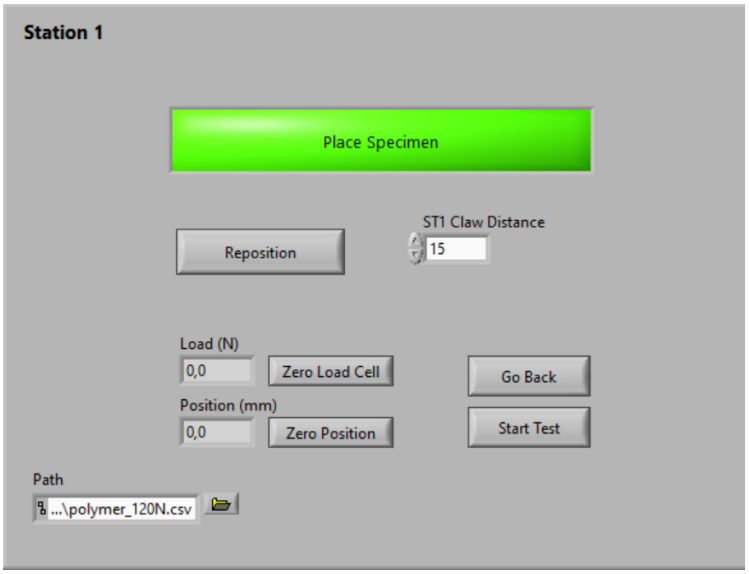

Figure 4.16: Positioning GUI menu- ready

4.5.5.6 Positioning: State 5

The station only is required to go through this state in case the "Reposition" button has been pressed. The VPPX valve is set to 3 bar and the directional valve is set to deliver the airflow to the upper chamber pressurized at 6 bar, making the cylinder descend.

Interface wise, the "Start test" button is disabled and greyed out and the display reads "Wait" in dark grey once again.

When the lower travel switch is activated, the process starts anew: the station travels back to state 0.

4.5.5.7 Positioning: State 6

The "Start test" button is pressed and the machine enters state 6. This state is mainly a preparing stage for the upcoming "Test in Progress" state. Some local and auxiliary variables which will be used in the next machine state are reset. Also the file with the creep test data is created: it is identified by the data and time of the commencing of the creep test; then, it presents a line heading the variables that will be measured and registered - "Elapsed Time (s)", "Measured Load (N)", "Desired Load (N)", "Position (mm)", as shown in Figure 4.17. Upon creating and saving the file data document for the first time, the machine is ready to begin the creep test.

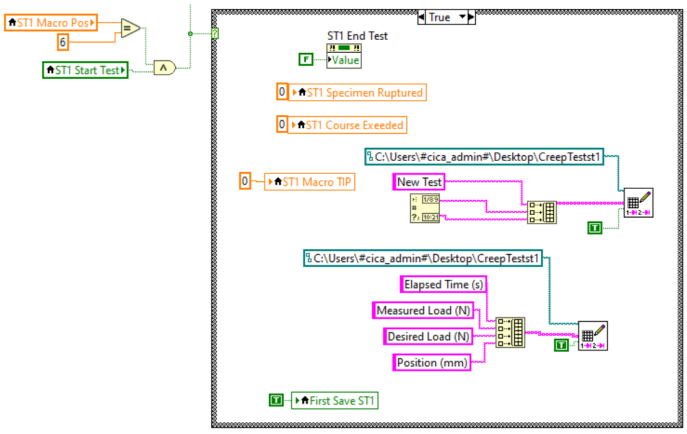

Figure 4.17: Positioning: State 6 block diagram

4.5.6 State: Test in Progress

The present state is the one where more actions and conditions are set simultaneously. Contrary to some previous states that (just like the program as a whole) function sequentially, "Test in Progress" is a more conditioned based state that can end in different ways due to different factors or results.

The interface of this state displays a chart of the displacement in function of time, the test time, the measured load by the load cells and a button that allows the user to end the test at any point he chooses (Figure 4.18).

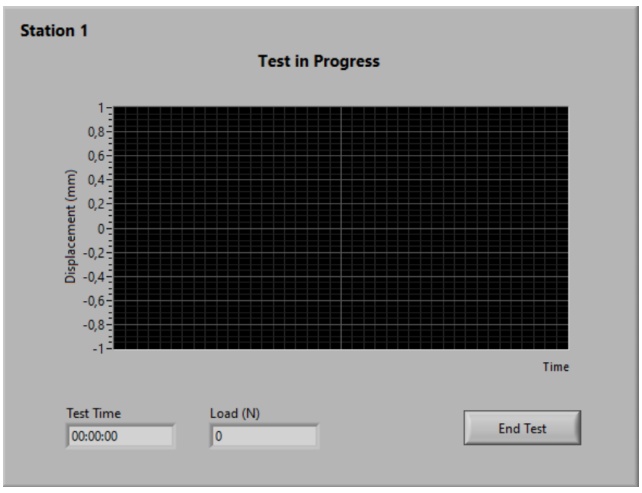

Figure 4.18: Test in progress GUI menu

From all the data being registered and displayed in the interface, only "Test time (s)" and "Load (N)" - measured Load - are being updated in real-time. The measured load is obtained by subtracting the weight of the upper assembly and specimen, which was previously measured, to the overall load measured by the load cells. This way, the data shown and recorded during the test takes into account only the load applied by the pressure of the upper

chamber of the cylinder. Before, measured load was obtained by subtracting the offset created when "zeroing" the load cells. This meant that during the tests, two specimens with different offsets would produce the same measured load in the interface when the absolute value of the load cells (that could be read in the "Debugging" panel) was different when should also be equal. The pre-compressive or pre-tensile stress applied when placing the specimen in the machine proved to have no influence when conducting the test, since the resulting force during said test was only the one created by the pressure in the upper chamber of the cylinder. The other parameters or variables are being recorded according to the sample rate chosen in the "Test Parameters" state. As shown in Figure 4.19, "Load (N)" and "Test time (s)" indicators are placed outside of the case structure, meaning they are permanently being displayed and their value updated during the "Test in Progress" state. The data that is being recorded as well as the chart that displays the displacement of the specimen through the time elapsed are contained in the case structure. The displacement values are multiplied by -1 because the cylinder is descending and the value measured by the cylinder is always lower compared to the initial point. This case structure is activated in regular intervals of time according to the sample rate chosen.

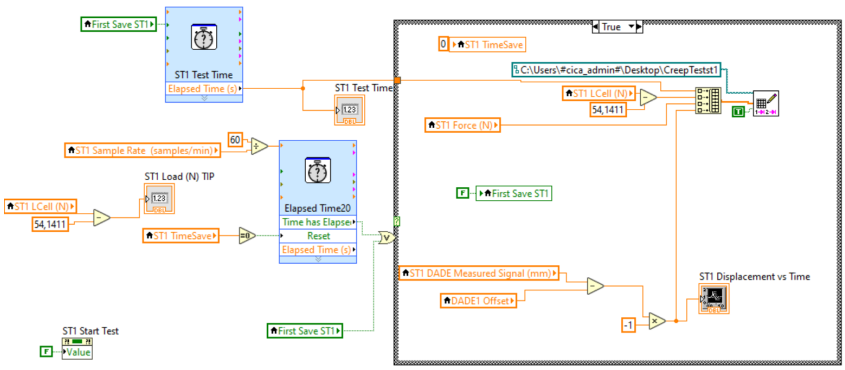

Figure 4.19: Data presented and stored during creep test

The data is not being recorded in real-time because creep tests can take hours, days or even weeks and the computational weight of saving all that data as well as process it after the test would be unbearable. Also it is unnecessary to have the same data saving rate for a test of two hours and a test of two days. The sample rate feature allows the user to preemptively choose, based on the length of the test, how often he wants to record creep test data.

As above mentioned when portraying the elements present in the GUI, the test can be ended at any point in time if the user decides to. However, this is only one of three conditions that can dictate the end of the creep test.

Reiterating, the first one is by clicking the "End Test" button on the interface and it is the only one that is user-dependant, this is, the other two are imposed by the software and hardware.

The second one results from the fracture of the specimen. In this case,

the response of the system isn't instantaneous. Although there is no tensile strength applied on the specimen, the pressure is the upper chamber of the cylinder will remain the same. Also, the load cell will continue to measure some load due to the weight of the remaining of the fractured specimen that is attached to the upper assembly of the station.

Once the VPPX pressure regulator valve is operating in internal mode a dependence between the VPPX setpoint and the measured load for that setpoint had to be found. In other words, there was a need to ensure that the pressure in the upper chamber of the cylinder guaranteed that the measured load due to that pressure would be equal to the desired load. Taking this factor into account, an equation that would relate the desired force and the pressure needed to exert that force was mandatory. The experimental process was conducted and is approached in the next chapter, resulting in the equation present in Figure 4.20, outside of the smaller case structure, and written below:

$$p = 0.0022 \times F - 0.0644, \tag{4.1}$$

where, p stands for Pressure [bar] and F stands for Force [N]. In the program, p is referred to as VPPX W+ (Setpoint) and F as Force (Desired Load).

Given that the dependence between the VPPX setpoint and the measured load is known and proven to work fairly well controlling and adjusting the VPPX pressure output, it will be used to end a test in case of specimen fracture.

After 30 s of the beginning of the test, which constitutes the initial load ramp application, if the measured load on the interface is below 60 of the expected load according to the VPPX measured pressure, the program acknowledges the specimen is fractured and the upper and lower claws (and assemblies) are now disconnected, putting an end to the test (Figure 4.20).

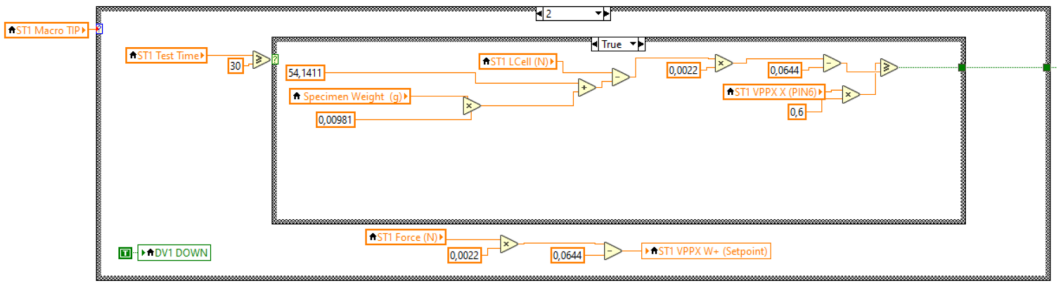

Figure 4.20: VPPX pressure- desired load equations and test ending conditions

The third condition is bounded to the available course limit. The course is limited by the lower travel limit switch. Once activated, it signals that the cylinder cannot move down any longer. So, even if the user did not choose to end the test or the specimen has not been fractured yet, the test will end due to the course have been exceeded (Figure 4.21). At this point, similar to the other cases, the directional valve will not allow airflow to the upper chamber, and the VPPX is set to 0 bar.

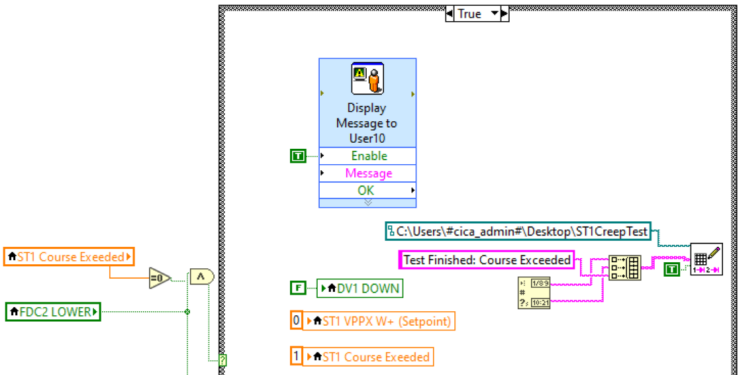

Figure 4.21: Course exceeded test ending condition

Once the test is finished, it is registered in the saved data file the condition responsible for the ending of the current creep test as well as the date and time at which such ending occurred. In the user interface, a message pops-up announcing the ending of the creep test and the reason behind that ending. Once the user confirms the test ending (by clicking "OK" in the displayed message box in the interface) the station transits to the "Test Finished" state.

4.5.7 State: Test Finished

After the test is concluded this menu displays a message, announcing to the user that the test has ended and the referring data has been saved. Right after the conclusion of the test, the test time is reset. This added condition proved useful to eliminate issues with the pressure compensation, that will be approached in the next chapter. Also orders the user to remove the specimen from the station in order to conclude the process and, eventually, start a new one (Figure 4.22).

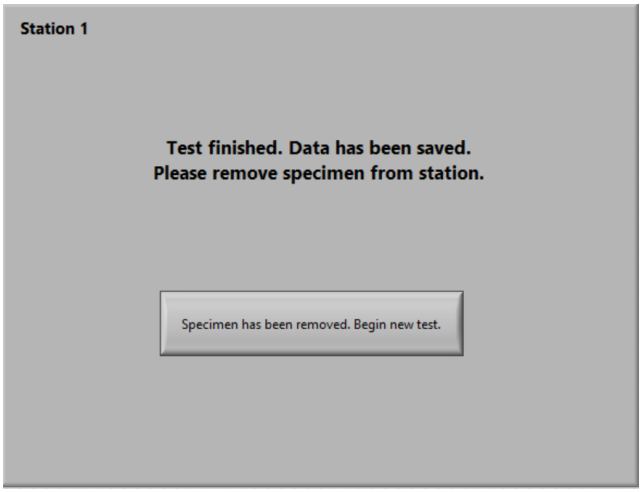

Figure 4.22: Test finished GUI menu

Clicking the button will inform the software that the specimen was indeed

removed and that the user intends to start a new test. Once this command is given by the user, the program checks the cylinder's encoder to ascertain if it is still referenced. If that is the case, then the VPPX is set to 4 bar and the directional valve's solenoid is actuated, allowing airflow to the upper chamber causing the cylinder's descent. When the cylinder reach the lower travel limit its sensor is actuated, resetting both VPPX (set to 0 bar) and the directional valve. At the same time, regarding the interface, the program shifts to the "Test Parameters" menu and awaits the user to input his desired parameters for a new test. Otherwise, if DADE measure value converter isn't still referenced the program transits to the referencing menu asking, once again, for the user to initiate the referencing procedure.

This state is composed by four substates allowing the sequential process that runs behind the interface. The inherent logic of this submachine is displayed in the schematics below (Figure 4.23).

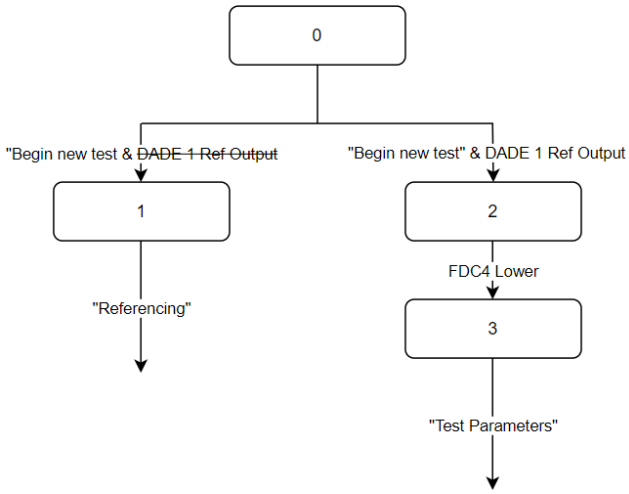

Figure 4.23: Schematics of "Test finished" substates

4.5.8 State: Emergency

The "Emergency" state is the last one of the system and it is unlike the previous ones. Firstly, this is not a sequential state of the machine. There can be hundreds or thousands of loops that do not require the emergency state. However, the command that is given to the system in order to initiate the emergency state overrides any other command or transition programmed, meaning that whatever the current state is or whatever code it is executing, the system transits to the emergency state (Figure 4.24). It can be referred as a priority state. Secondly, in this case if the emergency button is pressed, all three stations will change to emergency mode. This is a common safety feature that was included to prevent accidents or any harm to the user and allow him to take manual control (via computer) of some station elements, which will be discussed later.

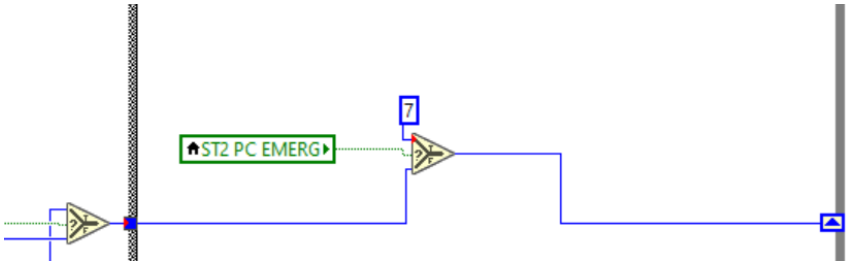

Figure 4.24: Triggering of the "Emergency" state

If either emergency buttons are pressed (physical or virtual), the directional valve is disengaged and the VPPX valve set to 0 bar, meaning the directional valve returns to its closed position and the regulator pressure valve does not allow airflow to the upper chamber. The PC EMERG variable is set to "True", triggering the PC EMERG relay, redundantly disengaging the directional valves.

When either the physical emergency button or the interface one are pressed, a warning message is displayed on the screen, telling the user that the system is currently on emergency mode and informing him he can take control of the stations, by clicking "Go to Emergency controls".

Once the user has disengaged the physical emergency button, the emergency control panel is opened. There, the user can rearrange the pressure values of the VPPXs and move the cylinder through the activation of the solenoids of the directional valves, via software (Figure 4.25). However, if the physical emergency button is not disengaged and the user intends to go to the emergency panel, the displayed message just pops up again, until that condition is satisfied. The control panel also has a LED display warning the user to be careful when manipulating the emergency controls.

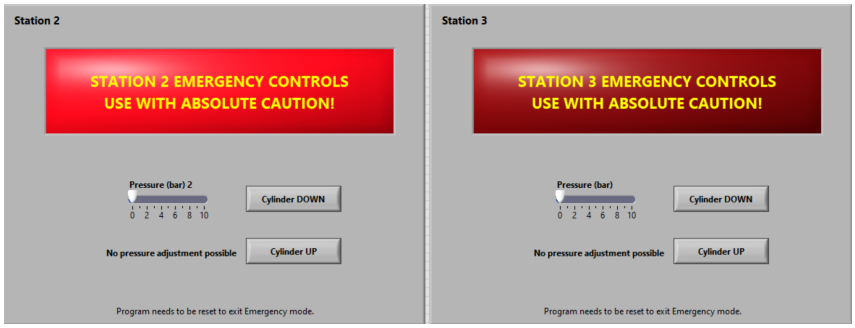

Figure 4.25: "Emergency" state GUI interface

Regarding the code running behind the interface, most of the controls are directly connected to the DAQ assistant, there is a case structure to allow the warning display to blink and one to disengage the PC EMERG relay (allowing the actuation of the directional valves).

Once the emergency is resolved, the program must reset. Such feature was included to prevent accidental exits of the emergency state. Since the

emergency state is common to all three stations, this means that even if only one station was malfunctioning, all tests must be stopped. Although it seems costly, the main priority is to guarantee the safety of the user.

4.6 Debugging menu

The debugging menu is a secondary panel where there are displayed all the important system variables (Figure 4.26).

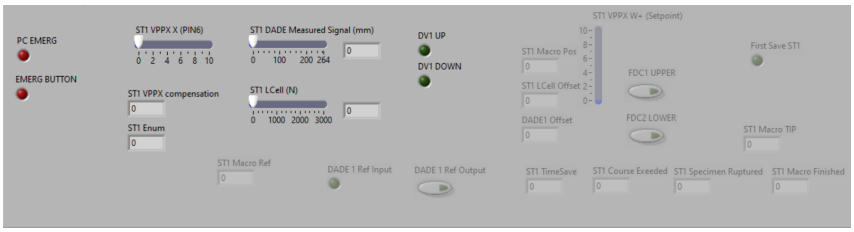

Figure 4.26: Debugging Interface

Auxiliary ones like the "MacroPos" and "MacroRef", that are responsible for the transitions between substates inside of, respectively, "Positioning" state and "Referencing" state as well as to keep track of which substate is currently running, are represented and exhibit an integer number that corresponds to the substate that the program is currently processing.

Other variables present in this interface are the digital ones. The directional valves as well as the emergency buttons, if triggered turn the LED light on. A similar process is applied to the travel limit switches. This allow the user to perceive if such variables are being activated at the right time in the machine's process.

The measured variables (pressure, load and displacement) are shown in real time in their absolute value (despite being "zeroed"), once these variables are directly connected to the DAQ and do not suffer any transformation in the machine's program. Such functionality helps providing immediate information about the test being conducted that can be valuable if some variable in the main interface is presenting inadequate or unexpected values.

The access to this secondary screen can be helpful to identify and locate errors that can affect the overall performance of the machine and to fasten its solution.

4.7 Post-Processing

Originally, the resulting data from a creep test performed in any of the stations that included the Time (s), Measured Load (N), Desired Load (N) and Displacement (mm) of any point saved according to the sample rate chosen by the user, was recorded in a notepad application. This was the default process of saving data through LabVIEW.

However, this system was not practical. One would have to open the notepad, copy everything to a program able to perform calculations, organize the data and plot charts evidencing relations between variables, like Excel or MatLab.

After performing some tests (which will be explored in the next chapter), it was decided to create a Post-Processing interface using Excel to facilitate the analysis of the tests performed. This solution was divided in two aspects: first, some changes were made to the LabVIEW code for each station in order to save the data directly to an Excel spreadsheet, instead of just saving it in a notepad. Second, an interface was created in Excel that copies the data recorded from a creep test and, based on that data, automatically fills tables and plots charts that resume and show the behaviour of such station during the creep test.

The Post-Processing interface contains two unfilled tables, two empty charts and a button that allows the user to copy data (Figure 4.27).

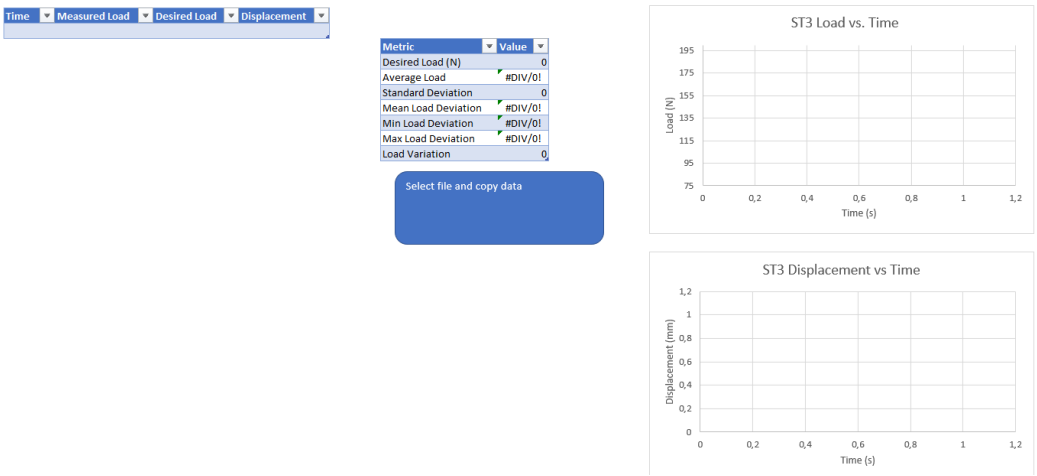

Figure 4.27: Post-processing Interface

When a creep test is finished and recorded in a spreadsheet, the user can open this template and copying the data by clicking the "Select file and copy data" button. After selecting the file to be copied, a macro programmed behind the button (Figure 4.28) opens said file, copies the data related to the creep test, closes the file and pastes it to the left table of the interface automatically.

```
(General)                                                    DeleteTableRows
'Apaga dados de uma tabela (fórmulas incluídas)
Sub DeleteTableRows(ByRef Table As ListObject)
    On Error Resume Next
    '~~> Clear Header Row `IF` it exists
    Table.DataBodyRange.Rows(1).ClearContents
    '~~> Delete all the other rows `IF `they exist
    Table.DataBodyRange.Offset(1, 0).Resize(Table.DataBodyRange.Rows.Count - 1, _
    Table.DataBodyRange.Columns.Count).Rows.Delete
    On Error GoTo 0
End Sub

Public Sub GetDados()
    Application.DisplayAlerts = False
    Dim wb As Workbook
    Dim FileToOpen As Variant

    Call DeleteTableRows(ThisWorkbook.Sheets("Sheet1").ListObjects("Table1"))

    FileToOpen = Application.GetOpenFilename _
    (Title:="Please Choose the RTCM File")

    If FileToOpen = False Then
        MsgBox "No file specified.", vbExclamation, "Duh!!!" ' Notification that nothing is chosen
        Exit Sub
    Else ' Load the file, copy the first sheet and paste it in active sheet ...
        ThisWorkbook.Activate
        'ThisWorkbook.ActiveSheet.Range("A1:Z65536").ClearContents

        Set wb = Workbooks.Open(FileToOpen)

        wb.Sheets("Folha1").Range("a1").CurrentRegion.Copy
        ThisWorkbook.ActiveSheet.Range("b3").PasteSpecial xlPasteValues

        wb.Close
        ThisWorkbook.Activate
        ThisWorkbook.Sheets("Sheet1").ListObjects("Table1").ListRows(1).Range.Delete
End If
Application.DisplayAlerts = True
```

Figure 4.28: Macro code

After copying the values to this template, it automatically fills the table that synthesizes the load performance during the creep test. Also, it automatically draws two graphics: the top one which relates the load applied with the test time and the bottom one which relates the displacement of the specimen also with the test time (Figure 4.29).

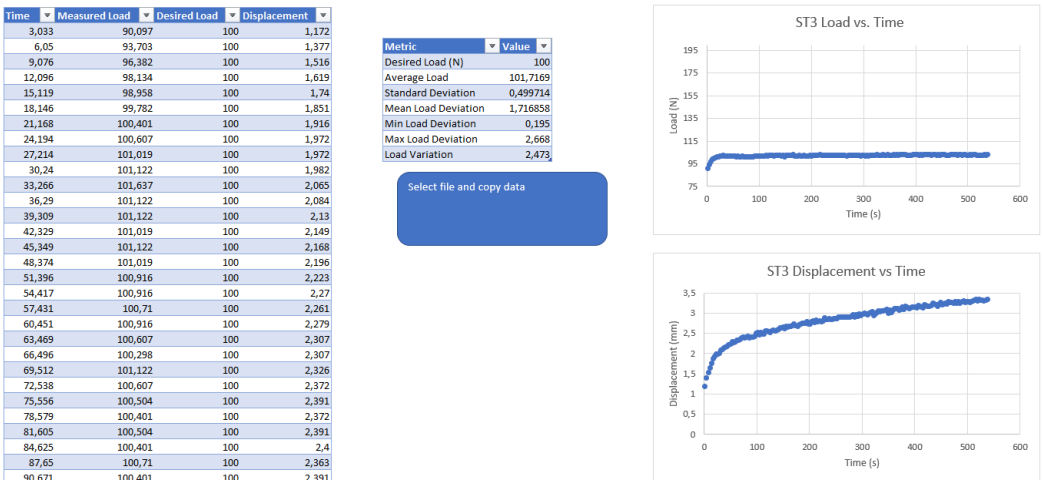

Figure 4.29: Post-processing Interface

Chapter 5
Test and Validation

This chapter addresses the overall testing of the machine elements. Both software and hardware must be verified to assess if there is malfunctions in the system. Tests to transducers and some other elements will be conducted so that when performing creep tests, the results obtained can be considered valid and reliable.

5.1 Software

The software testing is neither as methodical nor directed to a specific target. Instead, it is a verification of the functionality of the program as a whole. It can be considered a "black-box testing". A black-box testing is a method of software testing that examines the functionality of an application without peering into its internal structures or workings. In other words, specific knowledge of the code is not required. It is required to know what the software is supposed to do but not how it does it. This kind of functional analysis of the program is commonly used in state machines.

The procedure evaluates many aspects of the software: transitions, independence between stations regarding both interfaces and data recording, emergency controls, test ending conditions, variables assignments and timing (Figure 5.1). Overall, it assesses if the program does what it was designed for when it was designed to do it, independently and simultaneously for all three stations, if records the data obtained from the creep tests and saves them and if the interface responds to the user commands. All of this, while always maintaining as much safety as possible for the user.

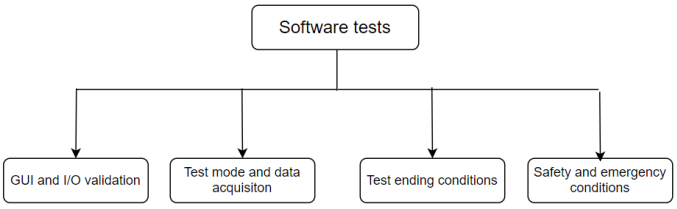

Figure 5.1: Overall schematics of the software test focus

The software tests performed rely or can be simplified in "Yes" or "No" questions asked by the tester to the program and verify the behavioral response given by it. Although in black box tests it is not required to have specific knowledge about the code, in this case that knowledge is required in order to change and force the program to execute what was designed. These tests were performed along the design of many phases of the machine's program.

The procedure created was divided into levels. The first one is the "Architecture" level (Figure 5.2). This level verifies if the general structure of the program is working properly. Firstly, it evaluates if the stations are able to run at the same time or if the program does not allow progress in one station if another one is already running. If that problem emerges, the structure of the code must be revised and altered. Secondly, it checks whether the transitions and interface inputs only set and activate the variables corresponding to that station. For instance, if a user in the first interface menu presses the button to start the referencing of the station 1 cylinders' encoders, then only that station should transit to the next state and interface menu. If there is cross information between stations, the DAQ connections and the labelling of variables have to be verified. After, the test focus on the second level.

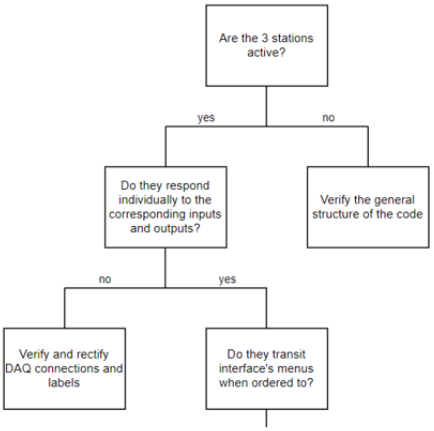

Figure 5.2: Architecture level schematics

The second level is the "Station" one. This level tests the internal process of each station, instead of the previous one that tests the external part of the code (Figure 5.3). The "Station" level, in simple terms, verifies the overall transitions between states and if those transitions occur only when they were designed to. Also, the set and reset of variables related to both hardware and virtual commands are checked to see if they are working as expected. If not, then the problem must be located in some DAQ connection or there is a fault in the variable logic. After this verification, the test transits to its third phase.

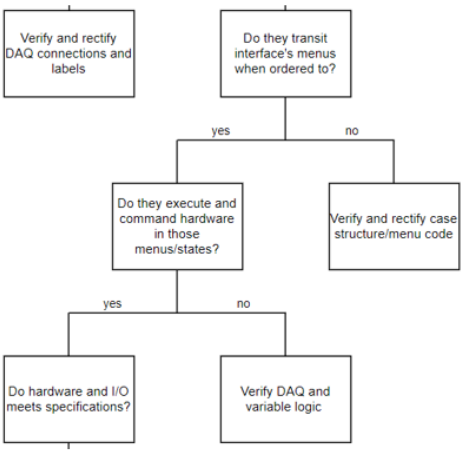

Figure 5.3: Station level schematics

The third phase is the "Conceptual and safety" level. After verifying if the code is running, it is important to ascertain if it is working as it was conceptual designed to (Figure 5.4). Overall, is the program positioning the claw according to the claw distance input? Is the airflow supplied to the cylinder's chambers according to the program requirements? Are the end testing conditions being met? This questions and many others that reflect the overall performance of the program are verified. In case that issues emerge, they can be related to code and that portion of code must be corrected or the conceptual model is wrong and new solutions have to be thought and implemented. At last, the safety conditions ("Emergency" state and "Hands of station" button) are tested to prove that the system is completely safe for the user.

This whole procedure was conducted and some corrections were made until the final and current state of the machine's program was reached.

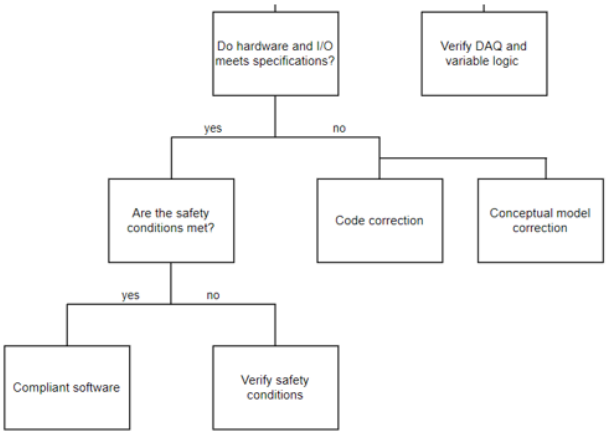

Figure 5.4: Conceptual and safety level schematics

5.2 Hardware

Besides software validation, there was the need to ensure that all the hardware was working properly. There was not a completely independent testing of hardware and software. When the program does not respond in the way it was planned to, it could be a coding mistake or it can be some equipment, or hardware that is faulting the system. For instance, in one of the software tests, ascertaining the independence of all stations while working at the same time, the interface of Station 2 did not transit form the "Referencing" state, while the others did. This happened not due to some coding error but because the lower travel limit switch on Station 2 was damaged.

In order to verify the condition of the hardware, a secondary program was developed. This program has two tabs, each containing the devices connected to the NI 6010 board and to the NI 6703 board, while displaying in real time those device's signals (Figures 5.5 and 5.6). The block diagram merely consists in having the controls and indicators displayed in the panel directly wired to the DAQ Assistant blocks (similarly to the structure of data acquisition built in the machine's program). Finally, it was designed a case structure dedicated to the saving and recording of the variables chosen to be studied. For instance, the load measured could be acquired and registered like in the developed program but also the voltage output from the load acquisition system could be saved and analyzed. The rate at which this data was saved and stored could be chosen and adapted to each situation and in order to save the elected data, one just has to toggle the switch in the second tab.

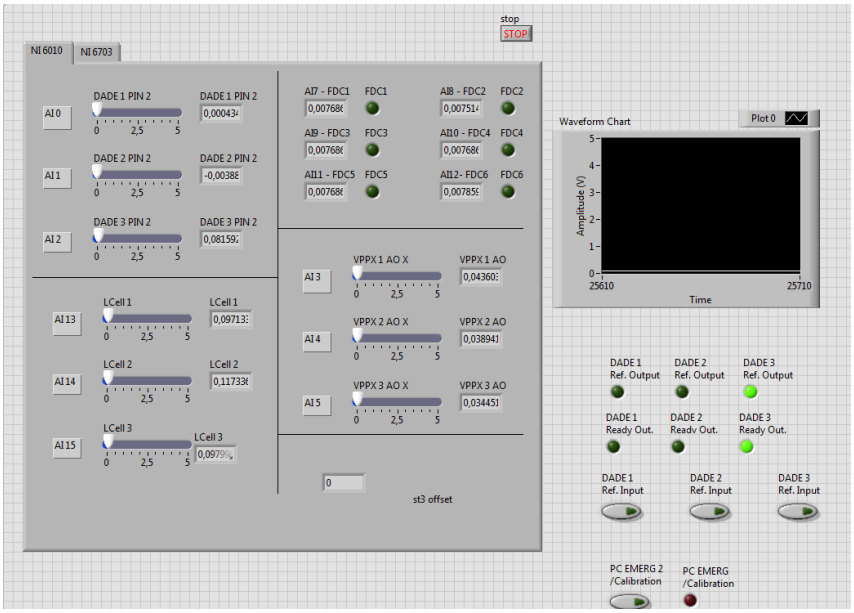

Figure 5.5: Software panel NI 6010

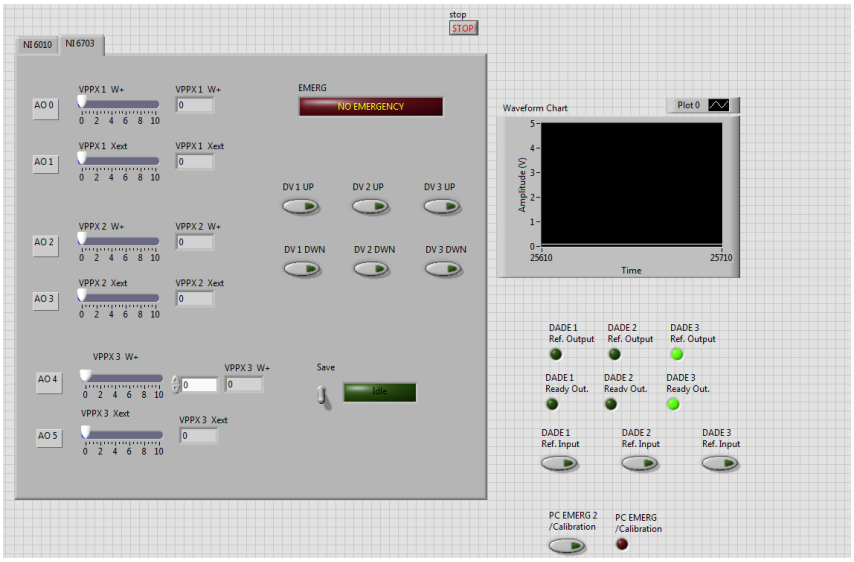

Figure 5.6: Software panel NI 6703

This program enabled the calibration of the DADE Measured Value Converter of the cylinders' encoders. Also, it allowed to verify if the signals from the hardware were being acquired by the software, easily indicating hardware malfunctions that usually were due to bad connections or damaged components of the electric circuit. Using this program, some connections of the pneumatic circuit were also altered and due to the output voltage of the lower travel limit switch from Station 2 being close to zero when the cylinder's piston was immobilized at the lowest point of the course, it was noticeable that the travel limit switch was damaged. Lastly, this application was used to perform the hardware tests, which include the transducers measurement (both load cells and encoders) as well as the VPPX setpoint and measured load dependence, that are described in the following subsections of the hardware validation.

5.2.1 Transducers Measurement

5.2.1.1 Load Cells

When converting voltage signal from the load cell to the actual load applied in the specimen, a theoretical approach was initially taken, as exposed in section 4.4 when portraying the DAQ system. Since the input range of the DAQ board varies from 0 to 10 V and the load cell measures loads between 0 and 3000 N, then a simple gain of 600 converts the voltage read in the software to the applied load value.

In order to verify if the load cells were calibrated and if the gain was correct an experimental procedure was designed (Figure 5.7).

First, it was necessary to weight the sets that function as the reference the measured values will be compared to. The sets were weighted in a calibrated scale, so that their mass would be as accurate and reliable as possible. By

multiplying the mass value by the acceleration of gravity, the sets (99.081 N, 179.935 N, 279.016 N and 316.506 N) were referenced.

After that, the weights were hang up on the station (one at a time for each station) for about two or more minutes while the program developed for testing was recording the values measured by the load cell in intervals of 50 ms.

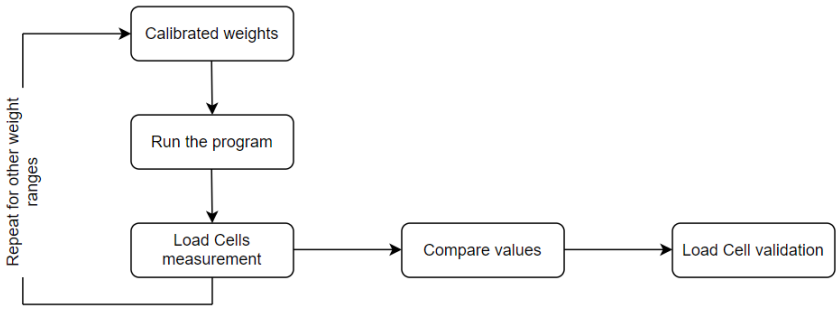

Figure 5.7: Load Cell measurement testing procedure

The first load cell measurement tests were actually performed with lighter weights. However, it was later realized that those tests could be counter-productive because of the non-linear zone that some transducers exhibit for both ends of their measuring range, being one of the reasons that the creep test has a lower limit of 100 N allowed in the software. Therefore, only the four sets numbered above were subjected to testing and the results of two of them - the 99.081 N and 179.935 N ones - for all three stations are shown in Tables 5.1 and 5.2 below.

Table 5.1: Load cell test for weight set of 99.081 N

	Station 1	Station 2	Station 3
Desired Load (N)	99.081	99.081	99.081
Average Load (N)	99.738	99.370	99.256
Standard Deviation	0.432	0.197	0.228
Mean Load Deviation	0.644	0.273	0.158
Min. Load Deviation	-0.471	-0.262	-0.576
Max. Load Deviation	1.514	0.887	0.887
Load Variation (N)	1.986	1.149	1.463

Table 5.2: Load cell test for weight set of 179.935 N

	Station 1	Station 2	Station 3
Desired Load (N)	179.935	179.935	179.935
Average Load (N)	181.435	180.543	180.243
Standard Deviation	0.393	0.274	0.238
Mean Load Deviation	0.833	0.338	0.171
Min. Load Deviation	0.303	-0.099	-0.157
Max. Load Deviation	1.398	0.879	0.575
Load Variation (N)	1.969	1.761	1.036

From the four sets only two were measured because analyzing the resulting data, some discrepancies from the desired values were pretty obvious. Firstly, the average load measured had a significant deviation from the weighted value, being the deviation in Station 1 the more severe: 0.644 to the 99.081 N set and 0.833 to the 179.935 N set. Secondly, the maximum load deviation (corresponding to the comparison between the weighted value and the maximum load value registered) as well as the minimum load deviation are rising compared to the weighted value as the load applied gets higher. The test of the 179.935 N set displays minimum load deviation that are practically zero - the lower registered value was equal to the weighted one - or, in the Station 1 case, the minimum load deviation was positive, meaning that all the load values registered were higher than the real weight of the set. Lastly, a load variation is quite clearly present in all stations. This variation does not have a visible pattern and it was associated with noise effects from the measuring system.

In order to solve both the first and second problems enumerated above, the same weights were hanged back up in the stations, but this time, instead of recording the load measured, the voltage from the load cell signals was directly measured (Table 5.3). This way, relating the real weight of the four sets with the average voltage output, a typical curve of the load cells was drawn (Figure 5.8).

Table 5.3: Voltage and real weight dependence

Voltage Output (V)	Set weight (N)
0.168	99.081
0.301	179.935
0.467	279.016
0.529	316.506

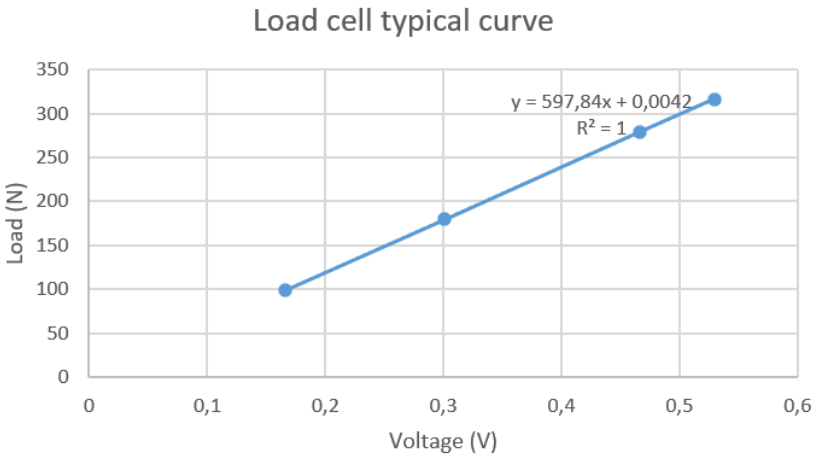

Figure 5.8: Station 1 Load Cell Typical Curve

The above mentioned table and typical curve belong to the load cell of Station 1. The remaining load cells from the other two stations were calibrated in the same way. The equations that translate the relation between the applied load and the output voltage are:

$$Station1 : F = 597.84V + 0.0042 \tag{5.1}$$

$$Station2 : F = 597.73V - 0.2509 \tag{5.2}$$

$$Station3 : F = 596.73V + 0.0323 \tag{5.3}$$

where, F stands for Load [N] and in the program it is referred as Measured Load [N] and V stands for Voltage [V].

After re-defining the load cell typical curve, the same weights were once again measured by recording the load applied in the station. The results are displayed in the Tables 5.4, 5.5, 5.6 and 5.7 below.

Table 5.4: Load cell test for weight set of 99.081 N

	Station 1	Station 2	Station 3
Desired Load (N)	99.081	99.081	99.081
Average Load (N)	99.026	98.934	99.114
Standard Deviation	0.419	0.429	0.231
Mean Load Deviation	-0.056	-0.148	0.033
Min. Load Deviation	-1.223	-0.770	-0.859
Max. Load Deviation	1.173	0.689	0.909
Load Variation (N)	2.374	1.444	1.752

Table 5.5: Load cell test for weight set of 179.935 N

	Station 1	Station 2	Station 3
Desired Load (N)	179.935	179.935	179.935
Average Load (N)	179.918	179.946	180.031
Standard Deviation	0.418	0.434	0.221
Mean Load Deviation	-0.010	0.006	0.053
Min. Load Deviation	-0.686	-0.330	-0.397
Max. Load Deviation	0.748	0.358	0.405
Load Variation (N)	2.581	1.238	1.442

Table 5.6: Load cell test for weight set of 279.016 N

	Station 1	Station 2	Station 3
Desired Load (N)	279.016	279.016	279.016
Average Load (N)	279.039	278.908	279.068
Standard Deviation	0.422	0.424	0.237
Mean Load Deviation	0.008	-0.039	0.019
Min. Load Deviation	-0.398	-0.285	-0.314
Max. Load Deviation	0.453	0.232	0.278
Load Variation (N)	2.374	1.445	1.649

Table 5.7: Load cell test for weight set of 316.506 N

	Station 1	Station 2	Station 3
Desired Load (N)	316.506	316.506	316.506
Average Load (N)	316.491	316.474	316.555
Standard Deviation	0.421	0.415	0.242
Mean Load Deviation	-0.005	-0.010	0.015
Min. Load Deviation	-0.421	-0.259	-0.271
Max. Load Deviation	0.394	0.230	0.249
Load Variation (N)	2.581	1.548	1.649

All four tables resuming the behaviour of the load measurement system are shown to better illustrate the obtained results and the improvements when compared to the first set of measurements.

The average mean deviation was approximately zero, except for one measurement in Station 2 (but the other measurements done in that station proved the correct calibration of the load measurement system). Besides that, the average load measured and, consequently, the mean load deviation oscillate between the real value not showing a linear increase or decrease as the load applied in the station rises. Also, the maximum and minimum deviations are approximate equal (in absolute value). This results are evidence that the offset and gain problems of the load cells measurement system were dealt with.

Despite, the variation due to the noise is still present, it can be overlooked since for the high number of data collected, the noise cancels itself out, having a null effect on the overall load read. A filter can, however, be applied in order to reduce the noise effects.

5.2.1.2 Encoders

Similar to the load cells, the encoders also have a equation that defines their theoretical behaviour. Such equation was already described in this dissertation, in section 3.3.2. The procedure followed is displayed below (Figure 5.9).

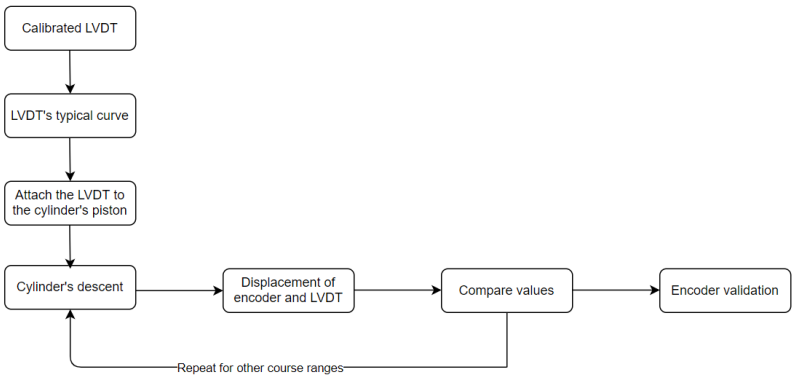

Figure 5.9: Schematics of encoders calibration

In order to evaluate the displacement measure of each encoder, it was decided to compare its output value to the one of a LVDT transducer (Linear Variable Differential Transformer). Its output voltage range is -5 V to 5V and, theoretically, corresponds to a 0 to 50 mm displacement. To discover the real relation between voltage output and displacement measured, the LVDT was put in a calibrated INSTRON machine. As the apparatus was ordered to descend, the INSTRON's BlueHill software was recording the displacement of the machine (and consequently the one of the LVDT that was "attached" to the machine) and the InstruNet software was recording the LVDT voltage output. Combining that information, it was possible to relate the voltage output of the LVDT and the displacement that occurred, drawing the LVDT typical curve (Figure 5.10).

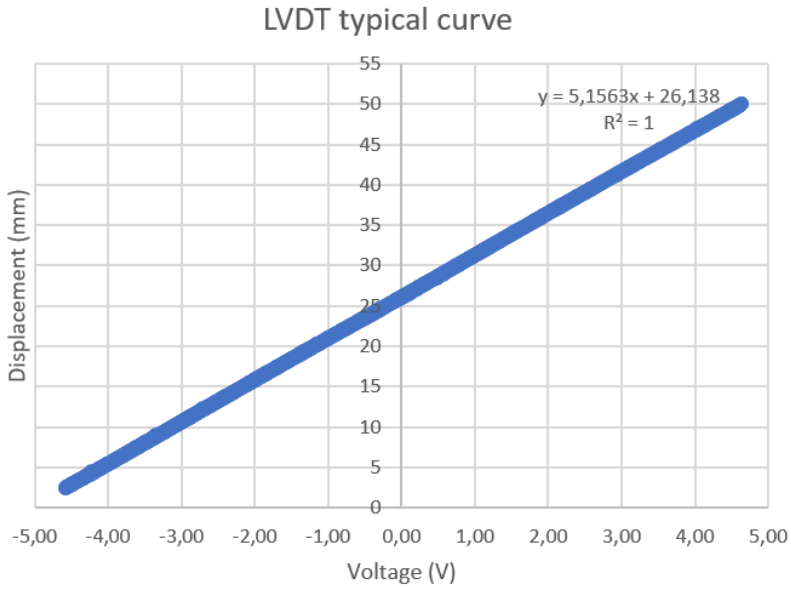

Figure 5.10: LVDT typical curve

The typical curve of the LVDT transducer can be described by:

$$d = 5.1563V - 26.138 \tag{5.4}$$

where d stands for displacement [mm] and V for voltage [V].

Now, the LVDT is ready to function as a reference for the displacement read by the encoders. The test was executed in three different levels of the work stroke available, defined as low, medium and high levels. The LVDT was landed on the top of the cylinder's piston and the cylinder was ordered to move down. While the cylinder descended, InstruNet was recording the LVDT's voltage output (that would be converted in displacement using the typical curve). At the same time, the cylinder's displacement was being recorded via software. All data were being recorded in 50 ms intervals. The values recorded are shown in Tables 5.8, 5.9 and 5.10.

Table 5.8: Low level encoder test results

Low Level	LVDT	ST1 Encoder
Initial Voltage (V)	-2.433	2.048
Final Voltage (V)	4.741	1.365
Initial Measured Point (mm)	13.594	107.621
Final Measured Point (mm)	50.582	70.845
Displacement (mm)	36.988	36.766

Table 5.9: Medium level encoder test results

Medium Level	LVDT	ST1 Encoder
Initial Voltage (V)	-4.228	3.467
Final Voltage (V)	4.636	2.622
Initial Measured Point (mm)	4.338	184.076
Final Measured Point (mm)	50.041	138.564
Displacement (mm)	45.703	45.512

Table 5.10: High level encoder test results

High Level	LVDT	ST1 Encoder
Initial Voltage (V)	-4.677	4.315
Final Voltage (V)	4.567	3.543
Initial Measured Point (mm)	7.780	229.802
Final Measured Point (mm)	49.686	188.216
Displacement (mm)	41.886	41.586

Although the encoder and the LVDT are measuring in opposite fashion, the interest of this procedure is to compare the displacement of both devices for the same elapsed time. The displacement deviation of the encoder is about 0.6 %. Despite not being a tremendous deviation from the actual value, some creep tests require a very precise displacement measure.

Assuming the linearity of the cylinder's encoders, a relation can be established between the displacement of the LVDT and the voltage output of the DADE. Such relation would be the encoder's new slope in its typical curve. The slopes for each level testes are displayed below.

$$m_{low} = 54.188[\text{mm/V}] \tag{5.5}$$

$$m_{medium} = 54.103[\text{mm/V}] \tag{5.6}$$

$$m_{high} = 54.267[\text{mm/V}] \tag{5.7}$$

where, m_{low}, m_{medium}, m_{high} stand for the slope obtained in the low, medium and high level, respectively.

Since there can only be one equation that describes the behaviour of the DADE and encoders, and, once again, assuming linearity through the whole range of the encoder, the average value of these 3 slopes was calculated and used as the new gain of the DADE, 5.9

$$m_{encoder1} = 54.186[\text{mm/V}], \tag{5.8}$$

where $m_{encoder1}$ is the average of the three slopes calculated previously and the value chosen to define the overall slope of the Station 1 encoder.

The same procedure was done for Station 3. The results are displayed below. While these tests were being conducted, one of the travel limit sensors stopped working, meaning that, at the time this dissertation is being written, the DADE of Station 2 is not yet calibrated.

$$m_{encoder3} = 54.225[\text{mm/V}], \tag{5.9}$$

where $m_{encoder3}$ is the average of the three slopes calculated previously and the value chosen to define the overall slope of the Station 1 encoder.

5.2.2 Applied load vs. pressure dependence

The load applied during a creep test is dependent of the pressure existent in the upper chamber of the cylinder. As the VPPX valves are currently configured for internal mode control, a constant reference value, the setpoint, has to be given to the pressure regulator valve. This issue was already mentioned in section 4.5.6 regarding the "Test in Progress" state of the machine.

A relation between the pressure inside of the upper chamber of the cylinder and the load applied on the specimen during the creep test had to be found. The simplest and most direct way would be to calculate the area of the chamber and divide the desired force by that area to calculate the pressure needed in the upper chamber. However, doing so, some friction forces, the lower assembly weight and other unknown factors could lead to a wrong relation between pressure and load applied.

A practical approach was taken: placing a specimen that suffers no deformation under the applied load, a steel specimen, and using the software created to test the hardware, some values were set for the VPPX input and the resulting load, as well as the setpoint value of the VPPX, were registered. The average load measured for each VPPX setpoint value is shown in Table 5.11 below.

Table 5.11: Relation between pressure and load applied

Average Load Measured (N)	VPPX setpoint (bar)
106.1528	0.1700
195.6729	0.3700
285.2488	0.5700
377.3163	0.7700
466.3728	0.9700

Using the points in the table above, a VPPX setpoint vs. Measured load curve was drawn, displaying an almost perfectly linear relation between the two parameters (Figure 5.11).

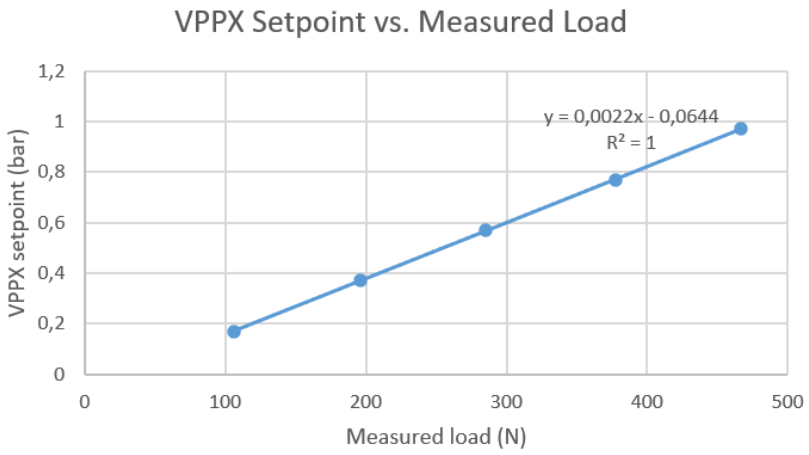

Figure 5.11: VPPX setpoint vs. Measured load curve

From the curve, it is possible to extrapolate the equation that defines the linear relation between the pressure regulator valve setpoint and the load measured by the load cells:

$$p = 0.0022 \times F - 0.0644 \tag{5.10}$$

where, p stands for Pressure [bar] and F stands for Force [N]. In the program, p is referred to as VPPX W+ Setpoint and F as Force (Desired Load).

This equation is numerically equal to the one in "Test in Progress" state of the machine, being responsible for calculating the pressure needed in the upper chamber of the cylinder based on the load desired by the user.

5.3 Constant Load Test

Creep tests are defined by maintaining a constant load applied during a certain amount of time. The time can vary from minutes to hours, days or even weeks. Given that, it is important to make sure the machine can endure applying a constant load.

In order to test the capability of the machine to exert a constant load during a large amount of time, a procedure of testing was created (Figure 5.12). A steel specimen, that does not present strain for the range of load values applied, is placed in a station of the creep test machine. A constant load is applied to that specimen and the data regarding the load measured is being recorded during the test. After the test finishes, the load measured values over time are analyzed, comparing the load measured to the desired load that was input in the system and how the applied load registered varied through the execution of the test. When both the difference between desired load and average measured load and the load variation throughout the test are minimal, it is safe to say that the machine can maintain a constant and

desired load applied over the specimen independently of the duration of the creep test.

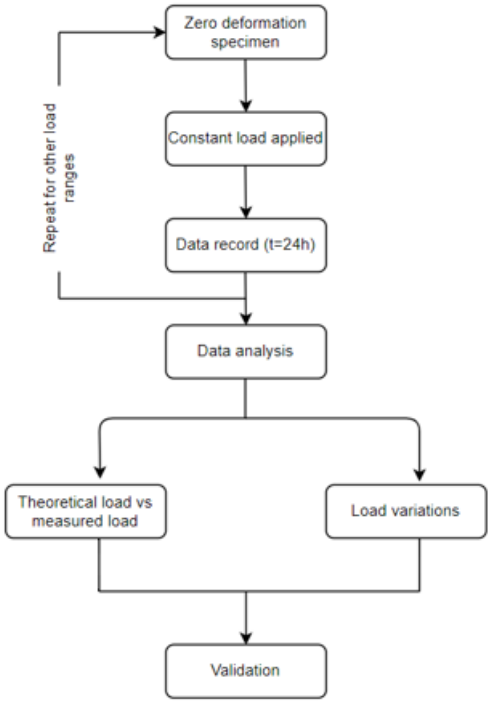

Figure 5.12: Schematics of the procedure for a constant load test

In order to test the ability of the machine to maintain a constant load applied to the specimen for hours, a steel specimen with little to none deformation, under the loading conditions, was placed in the machine and subjected to a 300 N load for about 16 hours. The results are displayed in the graphic (Figure 5.13).

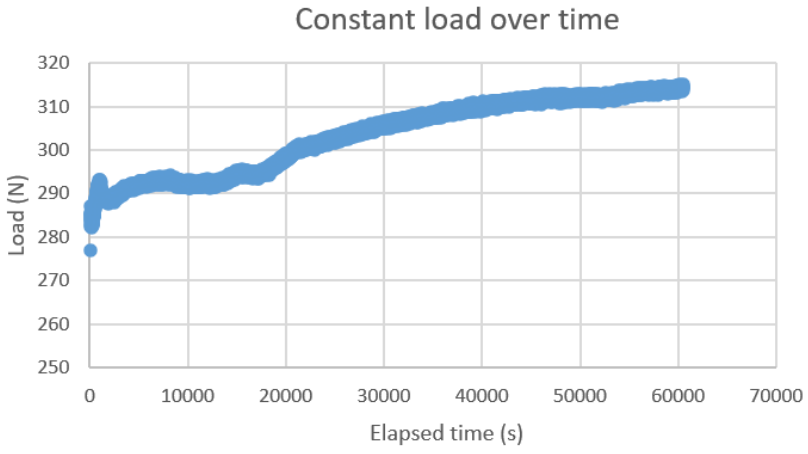

Figure 5.13: Constant load test

This graphic exhibits a lot of incongruities and a behaviour far away from expected. Table 5.12 summarizes the most important values taken from this specific test.

Table 5.12: Constant load test at 300 N

Desired Load (N)	300
Average Load (N)	303.3899
Mean Load Deviation	1.1300
Min. Load	282.2380
Max. Load	314.9630
Load Variation (N)	32.7250

There are several issues with the test results. First, the machine was not able to supply the desired load, being the initial load after the thirty seconds load ramp almost 20 N lower than the intended one. Secondly, the maximum load during the test was almost 315 N, resulting in a load envelope of approximately 33 N, faulting the objective of maintaining a constant load during said test. Also, the sharpest part of the graphic, where the rise in load applied is more accentuated, coincides with the night time period. For unknown reasons, the machine had even more difficulty exerting a constant pressure during that period of time. The test was repeated several times always displaying the same type of behaviour.

In order to fix the issue related to the initial pressure being lower than the desired one, the VPPX setpoint vs. Measured load curve was corrected, being the one shown in the previous section - the final and better performing one.

Since the VPPX is working on the internal mode, it can not regulate itself based on the load measured by the load cells. The first solution proposed was to create upper and lower limits that contained the measured load between that values. When the measured load reached one of those thresholds, an offset value should be added or subtracted to the VPPX setpoint value, correcting the pressure inside the upper chamber in order to maintain the load between that interval of loads.

A test, along the same lines of the previous one, was conducted desiring a load of 200 N. The thresholds were thought and imposed taking into account the noise of the load cells, being the offset 3 N. So, the range that the load values could vary (after 30 s) would be between 197 N and 203 N. If the load during the test reached 204 N, then the response would be subtracting an offset - 0.01 bar - to the VPPX setpoint value. The same logic was applied to the lower limit.

However, the response was far from ideal as shown in the graphic below (Figure 5.14).

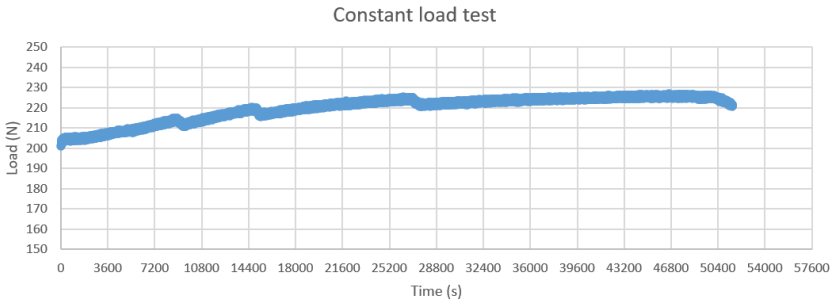

Figure 5.14: Constant load test

A new solution was proposed: a system of control that would continuously analyze the error between the desired load and the measured load and convert that difference (using the VPPX setpoint vs. Measured load slope) to a pressure value added or subtracted to the VPPX setpoint, if the error had negative value or positive value, respectively. This system was implemented in the "Test in Progress" state (Figure 5.15). Also, to negate effects of the noise, a gain of 3 was applied to the value that would be added or subtracted to the VPPX setpoint value. This gain was applied directly in the DAQ block (Figure 5.16).

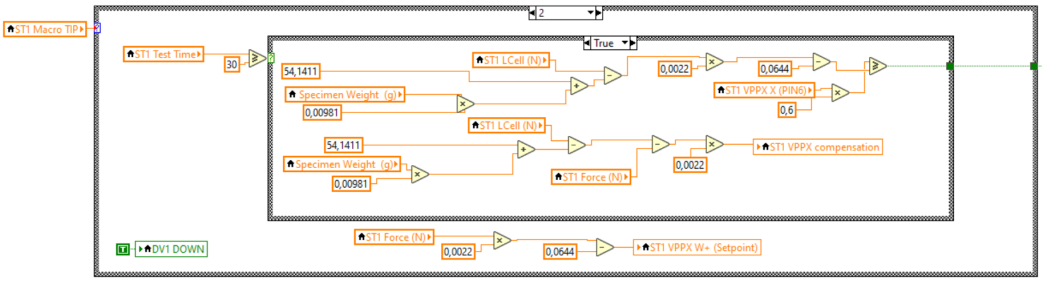

Figure 5.15: Pressure control system

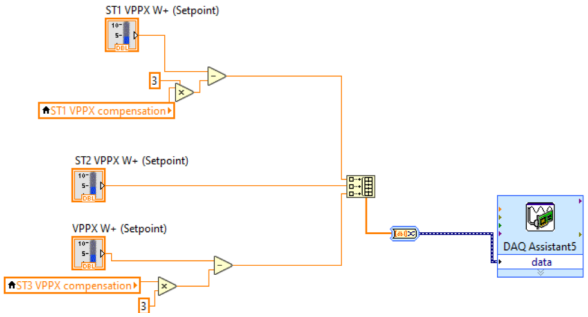

Figure 5.16: Pressure control system (DAQ)

Two tests were conducted after including this compensation on the system: the first one executed in station 1 for a desired load of 400 N and the

second one executed in station 3 for a desired load of 200 N (Figures 5.17 and 5.18).

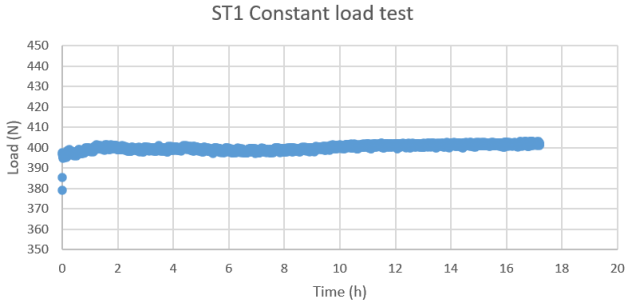

Figure 5.17: ST1 Constant load test

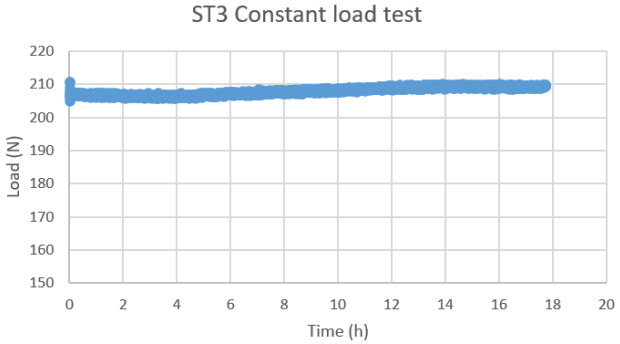

Figure 5.18: ST3 Constant load test

Both stations displayed huge improvements. The former solution reduced the load envelope but could not compensate a rise in load measured over time due to unknown reasons and mainly during night time. This real-time compensation included during the testing stage, reduced even more the load variation to acceptable values even when working overnight. The behaviour of both stations is shown in Table 5.13.

Table 5.13: Stations 1 and 3 constant load tests

	Station 1	Station 3
Desired Load (N)	400	200
Average Load (N)	400.000	207.922
Mean Load Deviation	0.000	3.961
Min. Load	394.875	204.987
Max. Load	403.031	210.242
Load Variation (N)	8.156	5.255
Time elapsed (h)	17.200	17.731

The table displays metrics in which the results are evaluated, being the

most important ones the averaged load (compared to the desired load), the load variation and time elapsed.

Starting by the latter, the time was approximately the same in both stations tests. More so, it was approximately the same during all the tests done to assess if the machine's stations were able to maintain a constant load applied during a large amount of time (always between 15 and 18 hours). Although in the experimental procedure schematics the time indicated is 24 h, that time is merely representative of the machine working continuously during a large period. In reality, despite the time span being a little shy of those 24 h, this does not constitute a problem or error. Simply, these tests were always conducted overnight because they were very time consuming, freeing the machine to perform other tests during the day.

Regarding the analysis of the results presented in the table, Station 1 was able to average a load applied exactly equal to the desired one.The load variation - 8.156 N - is significantly higher than station 3 - 5.255 - N, but even during the simple load cells tests, where a set of weights was hang up on the machine, the Station 1 already presented a much higher variation (in relative values) of load measured. However, this load envelope is acceptable since the VPPX valves are working on internal mode and Station 1 had the capability to apply a almost constant load that averaged exactly 400 N during over 17 hours. Station 3 exerted an average load almost 4% over the desired load - 207.922 N measured for a desired load of 200 N. Since the load cell for Station 3 was calibrated and the dependence between VPPX setpoint and load measured found as well as some creep tests or other experiments that were done interspersed with the constant load tests, in which station 3 was able to average loads that never deviated more than 5 N from the desired value, this mean load deviation was despised. The load envelope was pretty solid, only of 5.255 N in over 17h hours of continuous recording of data.

The results of this last iteration process of the constant load test were deemed good and each station is now prepared to perform creep tests in which the results can be reliable and accurate. Nevertheless, the implementation success of the pressure compensation system should be just a temporary solution that must be improved by reprogramming the valves to work in external mode.

5.4 Pressure Influence between stations

There was a concern regarding the fact that when the tests were not performed synchronously, the pressure variation when a station started a test or when it ended could affect the pressure and, consequently, the load applied to the specimen of another station in the middle of executing a creep test. Another concern was if the stations working simultaneously could reach the desired load as they did while working one at a time.

The main issues for the starting of the test were the positioning state where the upper chamber is allowed airflow to counter-pressure the lower cham-

ber pressure and the beginning of the test itself where the upper chamber is being pressurized according to the desired load input by the user. The main issue when a test is finished, specially when the specimen ruptured, is that the sudden pressure variation when the upper chamber is not fed airflow anymore could influence the pressure in the other stations.

In order to ascertain if the load remained constant during these particular events, a test was executed. Two similar polymer specimens with same dimensions, thickness of 1.5 mm and cut from the same film were placed in stations 1 and 3. The one in station 3 was placed first and subjected to a load of 100 N. A few minutes after the creep test in station 3 started, station 1 started positioning its lower claw in order to place the specimen. Four minutes after station 3 test begun, the specimen in station 1 was subjected to a load of 140 N. This load guaranteed that the specimen would rapidly rupture. In matter of fact, the test did not last longer than three minutes. Such test provided the answers to the concerns about the pressure influence between stations during the positioning, starting and ending of a test while another station is performing a creep test at the same time. The results are displayed in the graphic below (Figure 5.19).

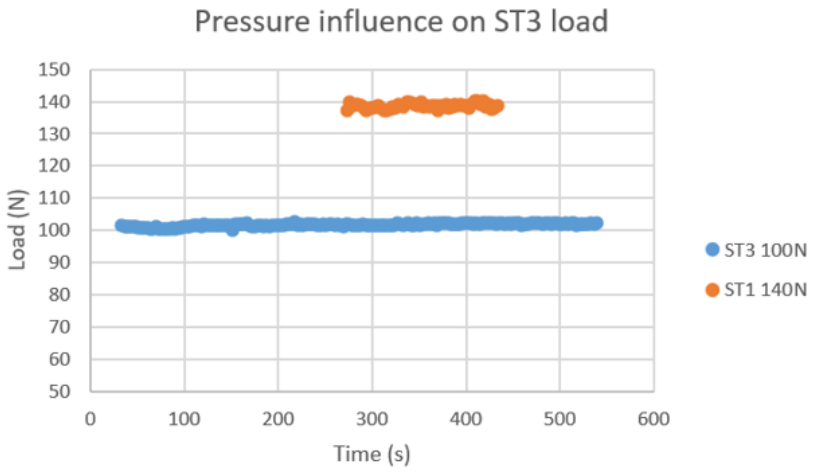

Figure 5.19: Pressure influence on Station 3

The inverted process was also put to test. Station 1 is exerting 100 N over a specimen and, after the beginning of that test, station 3 is positioned and four minutes after the test in station 1 has commenced, the creep test in station 3 begins, applying a constant load of 140 N. The results are shown in the following graphic (Figure 5.20).

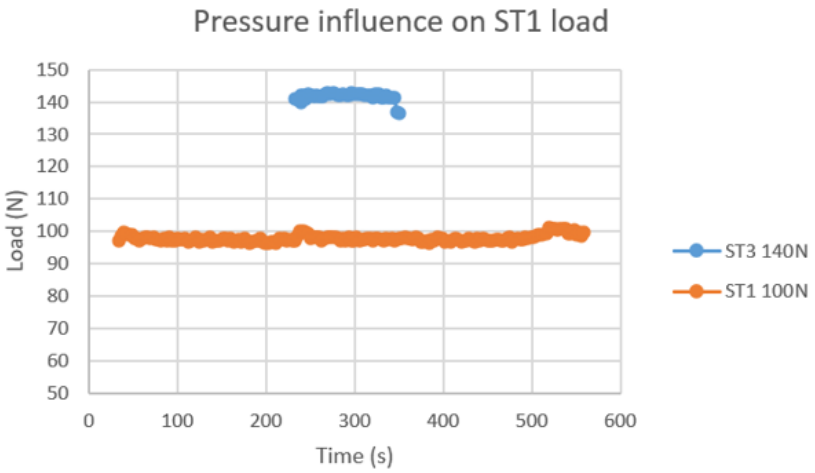

Figure 5.20: Pressure influence on Station 1

Station 3 showed no load variation during the "Positioning" process as well as during the start and finish of the station 1 creep test. Station 1 displayed a minor peak at the start of the station 3 test but it was almost immediately recovered and stabilized around the desired value (the pressure compensation system helped this immediate recovery). Also, both stations when working at the same were able to apply the desired load to the specimen. This two responses showed that the machine's stations are capable of working synchronously or asynchronously without being influenced by other working station.

Chapter 6
Creep Test

This section in divided in two subsections: the first one addresses creep tests performed using polymer specimens. These tests will allow the comparison of performance between both stations 1 and 3. Also, the creep test will also be performed in another machine and the results compared to the ones obtained in the machine under development. The second one covers the adhesive creep tests performed in the three-station creep machine and compares them to data recorded in literature regarding previous creep tests performed with the same adhesive.

6.1 Polymers Creep test

The polymer creep tests had two objectives: compare the performance of the stations and compare the test results from both stations with another machine to validate the results.

The machine used to compare the results is named GUNT WP 600 designed by Gunt Hamburg. This experimental unit demonstrates typical phenomena such as phases of different creep rates or temperature-dependent creep behaviour. The clean layout and simple operation mean the experimental sequence can be observed in all details and phases. Experiments can also be conducted below room temperature by means of a transparent temperature-controlled box with storage elements (Figure 6.1) [35].

In the experiment, the specimen is subjected to a constant tensile load at room temperature, once the tests in the developed machine are also done at room temperature and both machines are operating in the same room. The tensile load is generated by a lever and stepped weights that range from 5N (with no stepped weight) to 25N (with all the stepped weights), applying a constant load on the specimen between 50 N to 250 N. The elongation of the specimen over time is recorded by a LVDT (the same used in the encoders calibration test), using the LVDT typical curve to convert the voltage output to displacement.

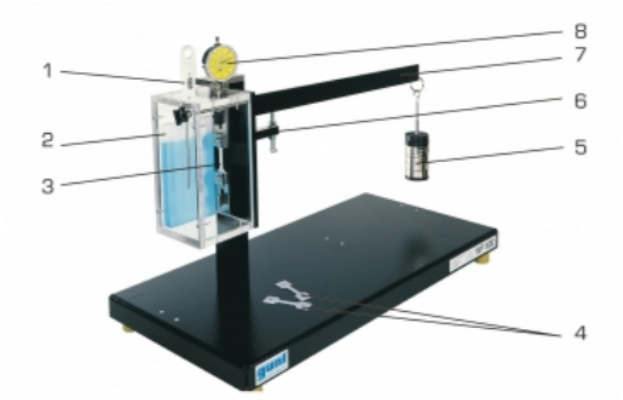

Figure 6.1: Gunt WP 600 experimental unit: 1-thermometer for temperature-controlled box, 2-storage element for cooling the specimen, 3-clamped specimen, 4-specimens, 5-weight, 6-adjustable stop for the lever, 7-lever,8-dial gauge [35]

Both stations and the GUNT WP 600 mechanical apparatus tested similar specimens (same dimensions, same thickness of 1.5 mm and cut from the same film in the same direction), subjecting them to 120 N (Figure 6.2).

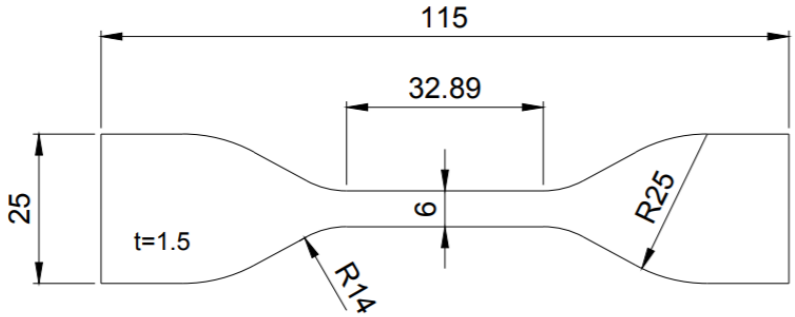

Figure 6.2: Polymer specimen (all dimensions in mm)

Before testing in the GUNT WP 600 machine, the creep tests were conducted in the three-station creep machine in both station 1 and station 3 aiming for a constant load applied of 120 N.

The tests performed on Station 1 (Figure 6.3) revealed a slight deviation from the desired value, being the average measured load value of 116.8 N, 116. 95 N and 118.3 N for tests 1, 2 and 3, respectively, while presenting a load envelope no greater than 6.5 N during the test (this variation will be lower once the filter is implemented and the VPPX is working on external mode). This slight deviation is considered normal and does not constitute an issue regarding the performance of the machine. Station 1 generated very good results both in repeatibility of the applied load and creep curve. Regarding the load aspect, this station was able to continuously and in all three tests apply, approximately, the same load to the specimen. Noticing the creep curves, the 3 curves display a similar displacement response of the three specimens subjected to test. The curves that describe specimens 1 and 2 creep behaviour, that were subjected

to almost equal loads, are overlapped which indicates the repeatibility of the machine in providing the load exerted over the specimen and the recording of the displacement suffered by the specimen. Specimen 3 suffered a displacement of 16 mm sooner (about 6 min), but the load applied was slightly bigger (about 1 N), which makes the creep curve draw expectable.

Figure 6.3: ST1 creep test curves for a load applied of 120 N

The tests performed on Station 3 (Figure 6.4) intended for a constant load of 120 N, averaged a measured load of 124 N, 124.2 N and 124.4 N, for tests 1, 2 and 3, respectively. Much like Station 1, this deviation is not considered abnormal or outside of the acceptable range. The load variation was always lower than 4.5 N (Station 3 usually displays lower load envelopes than Station 1). Although Station 3 caused a displacement of around 16 mm sooner than Station 1, such results are expected once the loads involved were bigger. The results in terms or repeatibility praised for Station 1 are also noticed in Station 3. The average load all three tests varied under 0.5 N, proving the ability of the machine to repeatedly subject the specimens to the same load. Two out of three tests show very similar behaviour regarding the displacement of the specimen over time (tests 2 and 3), while test 1 caused a creep curve that took slightly longer to reach 16 mm of displacement (under 5 min). Also, test 2 caused a creep curve marginally more accentuated than test 3 despite the average load measured being vaguely lower during test 2. Still, the all three creep curves display a similar behaviour and the two issues mentioned above may be related with thickness or area changes between specimens that were not controlled or intrinsic properties of the specimens which can not be controlled.

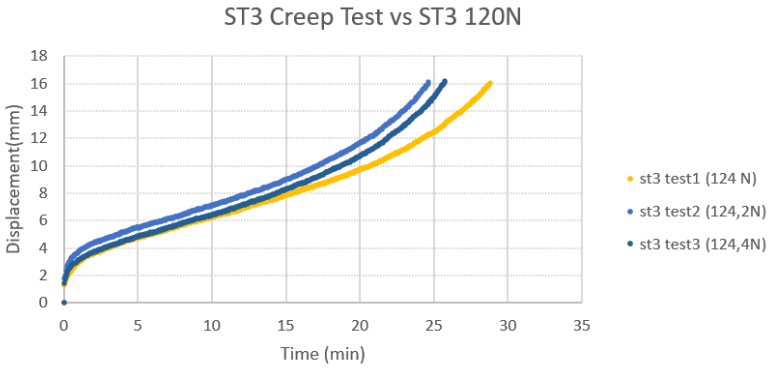

Figure 6.4: ST3 creep test curves for a load applied of 120 N

Since, when testing in the machine's stations intending a load applied of 120 N, there were slight deviations from the desired value: station 1 averaged load around the 117 N and station 3 averaged measured loads around 124 N, the experimental procedure was adapted. Station 1 results were compared to tests performed in the GUNT WP 600 machine for 115 N and station 3 results were compared to 125 N GUNT WP 600 creep tests.

Analyzing the results of the tests performed on the GUNT WP 600 experimental unit (Figure 6.5, one can see that the behaviour of the tests is somewhat different. The load applied was objectively the same: 115 N. However, the creep curves the test produced are quite different: the initial elongation of the specimen is lower in test but the slope of the curve is bigger, resulting in both stations, coincidentally, reach about 14 mm of deformation for, approximately, the same elapsed time. Comparing to the results obtained in Station 1 (Figure 6.3), the elapsed time to reach about the same elongation has almost doubled. This results can be explained by one of two factors: the slight difference in load applied or a bad calibration of the station components. In order to assess the source of the results deviation, another test was performed in Station 1 aiming for constant load applied of 115 N. Station 1 averaged a measured load of 114.7 N and when compared to the curves produced by the GUNT WP 600 experimental unit, it is noticeable that Station 1 curve is less accentuated than the other two and it took more time for the specimen to reach the same elongation, meaning the doubling of time elapsed was due to the load applied being slightly minor.

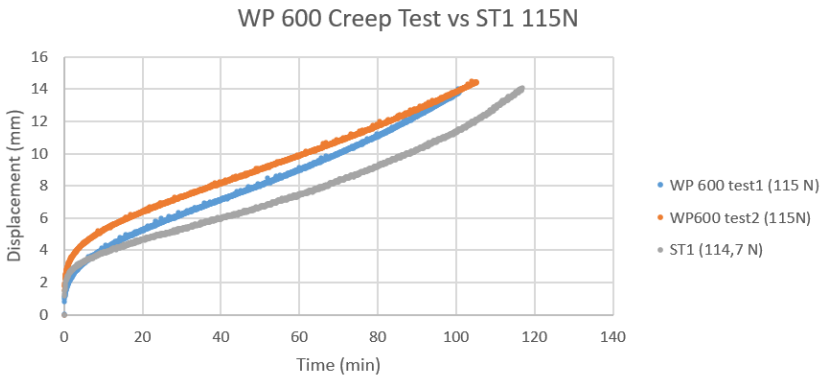

Figure 6.5: WP 600 creep test curves for a load applied of 115 N

The GUNT WP 600 apparatus was then used to perform tests of 125 N in order to compare the results with the ones obtained in Station 3 (Figure 6.6. Two of the tests (1 and 3) displayed very similar curves, while test 2 produced a different curve, where the specimen suffered a bigger displacement at the beginning but after that initial elongation, its creep rate was quite lower. This results show that even testing similar specimens with the same load applied, the creep curves can be sometimes different due to physical or structural irregularities of the specimen itself. Comparing to the curves of the Station 3 tested specimens, one can notice that the ones obtained by Station 3 are more identical than the ones produced by the experimental unit which shows a good testing behaviour of the developed machine.

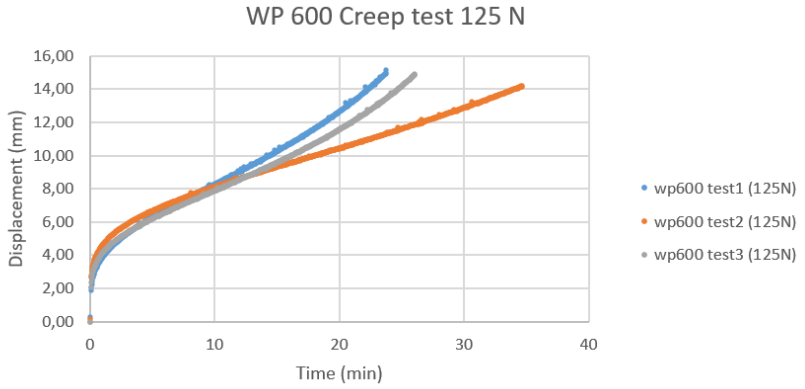

Figure 6.6: WP 600 creep test curves for a load applied of 125 N

The curves obtained by both Station 3 and the WP 600 machine for creep tests where the specimens were subjected to a load of 125 N are displayed in Figure 6.7. This Figure contains only the more similar curves obtained by either machine, since the goal is to compare the results obtained to assess the capability of the developed machine to produce reliable results (and in order to do that, there is no need to display the curve obtained by the WP 600 in test 2, for example). It is noticeable that all curves display a similar behaviour,

being the major difference the initial displacement of the specimens subjected to test in the GUNT WP 600 experimental unit which can be explained by the immediate load applied of 125 N while in Station 3 there is a load ramp that lasts 30s. All specimens, independently of where they were tested suffered the same elongation in about the same time, demonstrating the machine capability to produce reliable and repeatable results.

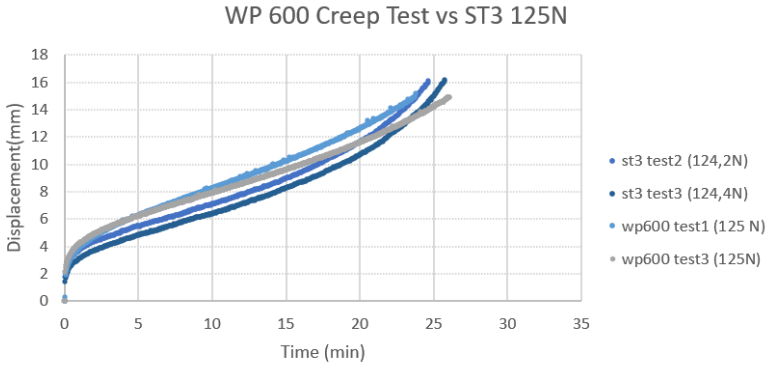

Figure 6.7: WP 600 and ST3 creep test curves

In order to test the machine's performance for other load range and to compare the test results between the two working stations, a new set of creep tests were executed. This time, instead of being limited by the displacement the WP 600 apparatus was capable of, it was decided to set a time limit of 30 minutes and compare the displacement suffered by the specimens in the set of similar tests. The specimens used were geometrically equal to the ones used in the previous tests, except the thickness of these specimens was 2 mm, which allowed to raise the load applied to 160 N. The summary of this set of tests is shown in Table 6.1.

Table 6.1: Polymer creep test results for 160 N

	ST1 Specimen1	ST1 Specimen 2	ST3 Specimen 1	ST3 Specimen 2
Desired Load (N)	160	160	160	160
Average Load (N)	159.537	159,207	162.408	162.247
Load Variation (N)	6.401	5.162	4.328	5.667
Displacement (mm)	8.224	7.629	9.052	9.536
Test duration (min)	30.246	30.3372	30.175	30.432

Once again, both stations were able to produce repeatable results. Although the average load remained somewhat deviated from the desired one (159.2 N for station 1 and 162.4 N for station 3), the loads averaged by both stations are perfectly acceptable and are closer to the desired value than the ones obtained in the creep tests performed at 120 N. The load envelope remained equal to prior tests (independently of the duration of such tests) and can one more time be considered as natural noise of the machine acquisition systems.

The displacement of the tested specimens for the same station are quite similar and such variation is expected. Between stations the difference obtained between measured displacement values can be explained by the slight average load difference between the two stations. In the following graphic, the creep curves obtained in this set of test are displayed (Figure 6.8).

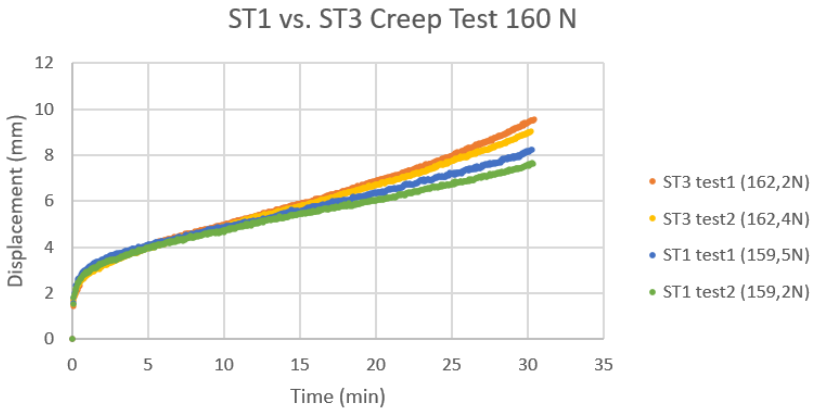

Figure 6.8: ST1 and ST3 creep test curves for a load applied of 160 N

By observing the graphic, one can confirm the similar creep behaviour in all four tests, especially, in the primary creep phase. The curves corresponding to creep tests performed in the same station are practically equal and the difference between both stations' tests that can be observed mostly after the 15 minute mark, where the curves that belong to the station 3 tests have a more accentuated slope can be explained by the load applied by both stations. Despite that variation, the results show that both stations can repeatedly exert the same load, provoking a very similar displacement and creep curve to similar specimens.

After conducting all the above described tests as well as analyzing their results, it can be concluded that the machine was successful in exerting a load very close to the desired one and maintain it approximately constant during the creep test execution. Also, it was able to perform this task repetitively. Both stations displayed similar results when asked to perform the same task. At last, both stations of the machine were able to produce results that were found reliable when compared to another machine, even having more repetitive results than the external machine. The machine can then be validated as it is working properly and producing reliable, repetitive and accurate results. Nevertheless, some tests using adhesives were conducted to further validate the functioning of the developed machine.

6.2 Adhesive creep tests

The method of comparison used for the adhesive creep tests is different than the one used in the previous section: in the current section, the results

will be compared with the ones obtained and presented [36].

Since the results of the above mentioned article are being used as reference, the preparation of the bulk specimens subjected to that test was strictly followed [36]. The adhesive used was an epoxy with the trade name of Araldite 2011, Salt Lake City, Utah, EUA. This is a two-component epoxy adhesive (AW106/HV953U). In [36], it is described the method of preparation of graphene enforced epoxy specimens. However, this dissertation will only provide a comparison with the neat epoxy specimens, meaning the preparation was adjusted, following every step described, except the ones that refer to the graphene (Figure 6.9).

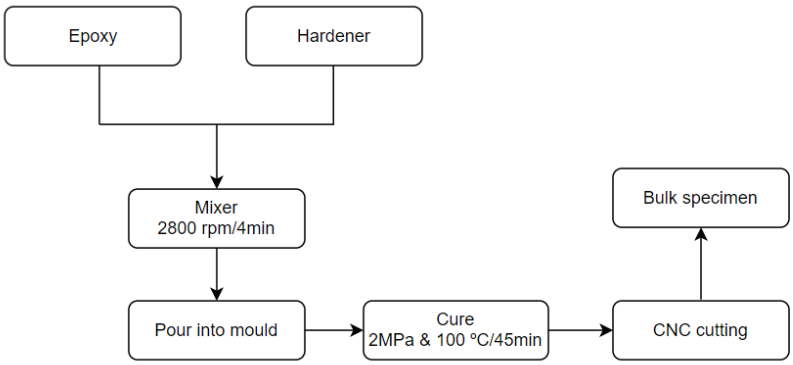

Figure 6.9: Adhesive specimen preparation schematics

The epoxy and the hardener were mixed using a centrifuge mixer for 4 min at 2800 r/min, after being weighted in proportion of 0.8 kg of hardener for each kg of epoxy adhesive. After this step, the mixture of epoxy and hardener was considered to be ready for pouring inside a rectangular mold, equipped with a silicone rubber frame. In order to obtain high-quality samples without any air bubbles and voids, the mold was first pre-heated in a hot plate press machine at 60°C. Following the pre-heating of the mold, the adhesive mixture was poured into the mold and spread evenly throughout the mold. Then, the mold was placed in a hot plate press machine under 2 MPa of pressure for 45 min at a temperature of 100°C to ensure the complete curing process. This procedure lowered the viscosity of the adhesive and, due to the high curing pressure, removed some of the trapped air, leading to a practically void free and high-quality adhesive plate in the most areas. The full-cure of an epoxy mixture takes between seven and fourteen days, despite presenting adequate strength for further assembly or packaging in just a few hours. The full-cure time interval was taken into account, looking to minimize all the possible differences in the manufacturing of the epoxy bulk specimens [36]. The bulk samples with the uniform thickness of 2 mm were obtained from the cured plates of the epoxy adhesive after cutting through the shown dumbbell shape geometry by a computer numerical control machine (Figure 6.13).

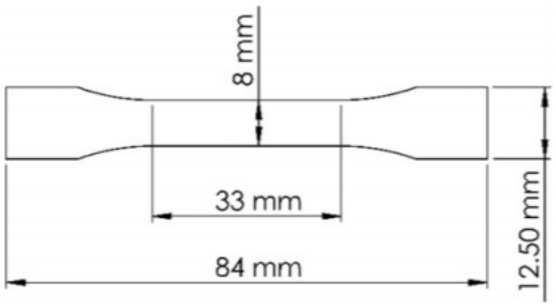

Figure 6.10: Bulk specimen geometry [36]

In [36], the creep test was performed applying a direct weight that resulted in the load that the specimen was subjected to, while measuring the displacement using an extensometer attached to the sample, recording the total strain of the bulk every 2 s.

The creep tests were conducted at three levels of constant load applied: 70 N, 150 N and 220 N which correspond to stress levels of 4.4 MPa, 9.4 MPa and 13.8 MPa, respectively. The stress values result from the load applied per initial cross section area, because during the test the load remains constant but the stress raises when the cross section area decreases. However, due to the amount of time and preparation needed to manufacture the epoxy bulk specimens, the fact that the machine only performs creep tests where the load applied is superior to 100 N and tests around 150 N were already conducted, the developed machine will only perform the creep test of the highest level of load applied: 220 N. The results obtained in the previous study of the creep phenomenon for this particular epoxy adhesive when subjected to a constant load of 220 N are displayed in Figure 6.11 below.

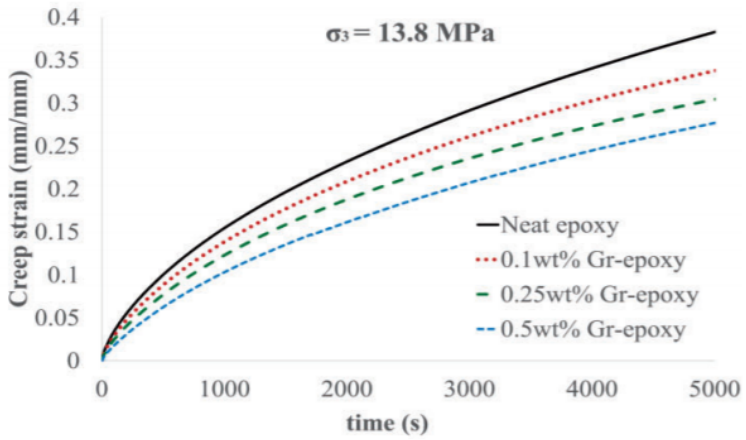

Figure 6.11: Creep strain curves of the epoxy for a load of 220 N [36]

The graphic presents several creep curves. The only one of interest to this dissertation is the full black one referent to the neat epoxy. This graphic, unlike

the ones presented in the previous section, is not a dependence of displacement in function of time but a relation of strain in function of time. The strain can be defined as the change in length per unit of the original length, as shown in the following equation:

$$e = \frac{\Delta L}{L}, \tag{6.1}$$

where e stands for strain [mm/mm] and L stands for length [mm].

Also, since the graphic is shown regarding the stress value and these specimens, contrarily to the polymer ones, had to be manufactured (and could, for instance, not possess the same thickness of 2 mm, a control of the cross section of all the specimens used was done (Table 6.2).

Table 6.2: Adhesive bulk specimen characteristics

	ST1 Specimen1	ST1 Specimen 2	ST3 Specimen 1	ST3 Specimen 2
Thickness (mm)	2.10	2.00	2.10	2.10
Width (mm)	8.05	8.00	8.05	8.10
Load (N)	220	220	220	220
Stress (MPa)	13.01	13.75	13.01	12.93
Air bubbles	Two(small)	Two(small)	Two(small)	One(small)

The creep tests were performed and the results are displayed in Figure 6.12 . Both stations were able to produce repeatable results regarding load applied. Intending for a constant load of 220 N, Station 1 executed tests 1 and 2 averaging exerted loads of 218.8 N and 219.1 N, respectively. Station 3 averaged in tests 1 and 2, a load applied of 222.4 N and 222.6 N, respectively. Regarding the load envelope, both Station 1 tests presented a load variation of about 6.5 N. As for Station 3, the first test presented a load envelope of 5.3 N and the load applied on the second one varied under 3.7 N. Once again, both stations are able to exert a constant load very similar to the desired one and maintaining it throughout the creep test, showing acceptable load envelopes. More so, both stations are able to continuously exert equal values of load applied (218.8 N and 219.1 N for Station 1 and 222.4 N and 222.6 N for Station 3), which shows the capability of the machine to supply and maintain very similar load values from creep test to creep test. The machine continues displaying repeatibility in terms of load applied.

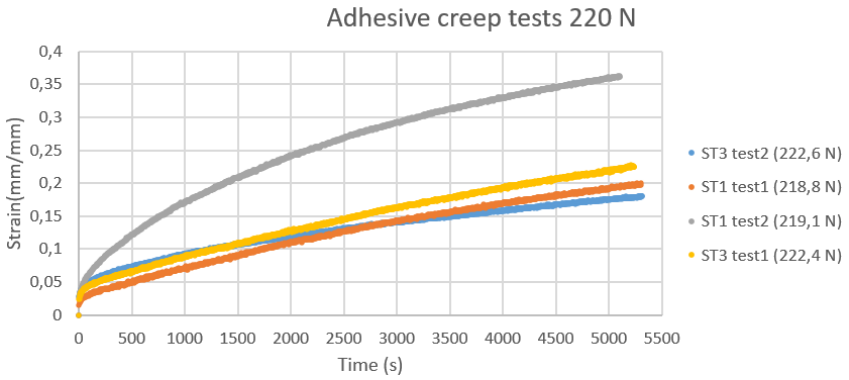

Figure 6.12: ST1 and ST3 creep tests for 220 N

The creep curves produced did not meet the expectations. First, three of those curves ("ST1 test1", "ST3 test1" and "ST3 test2") show strains revolving around 0.2, when in [36] the strain obtained was about 0.4. Analyzing those 3 curves, the curves for both stations first test are almost parallel, being the specimen on Station 3 the one who suffered greater displacement, which is perfectly acceptable once it was under more 3.5N of load applied than the one in Station 1. Station 3 test for 222.6 N suffered a bit less strain, while being under more load than the two previously discussed tests. This can be explained by the difference in dimensions, the presence of air bubbles or intrinsic properties of the specimen itself. However, the curves are still similar and the results were deemed good. The second test performed in Station 1 produced a curve similar to [36], almost doubling the strain of the other three curves. There is not a logical explanation for this, except perhaps the specimen presents some frailties that went unnoticed. A more likely explanation is the two adhesive plates possess different properties. Due to the mold limitations, only one adhesive plate can be prepared at a time. The two plates were manufactured in different days and even following carefully the preparation guidelines in [36], the curing process or the adhesive and hardener mixing proportions, could affect the strength of the adhesive plate. When the specimens were cut in the workshop, a differentiation of plates was not made, meaning tracking which specimens belong to each plate was not possible. One can argue that the first three specimens described belong to one plate and the other one belongs to another plate. The workshop provided eight bulk specimens. However, when measuring the specimens before testing, only seven could be counted. Four of them were used in the developed machine, one was used in a tensile test that will be approached later in this sub-chapter and two were meant to be used in the WP 600 GUNT experimental machine in order to eliminate any doubt regarding the reliability of the results. However, those specimens fractured by their fixing hole when put placed in the machine (Figure 6.13). Perhaps, the fixing hole was to big when compared to the dimensions of the specimen. This issue prevented the comparison between machine in order to ascertain the accuracy of the results.

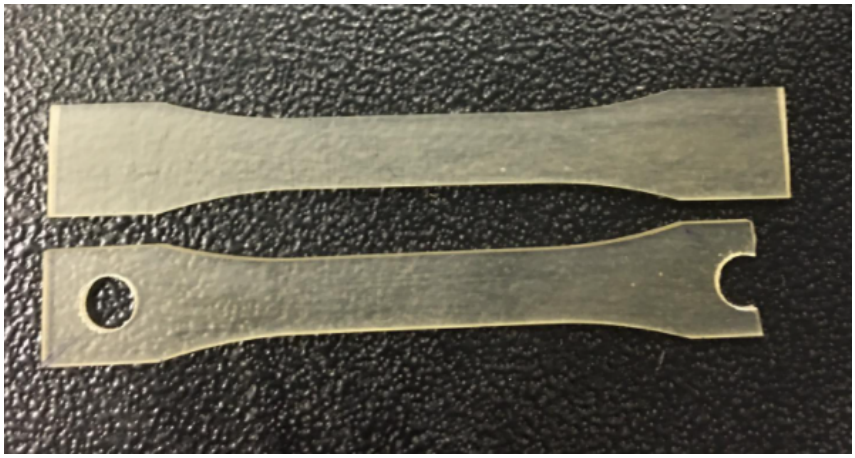

Figure 6.13: Bulk specimens (top: regular, bottom: broken

Once the test results did not meet the expectations, an analysis about the stress of the adhesive was conducted. First, the tensile test described in [36] was studied. The bulk samples were subjected to tensile testing following, while an Instron extensometer with an accuracy of ±0.5% and 25 mm of gauge length was used to measure the strain during the test. The ambient temperature was 27°C and the loading speed was 5 mm/min for all the specimens under simple tensile testing [36]. The results are displayed below (Figure 6.14).

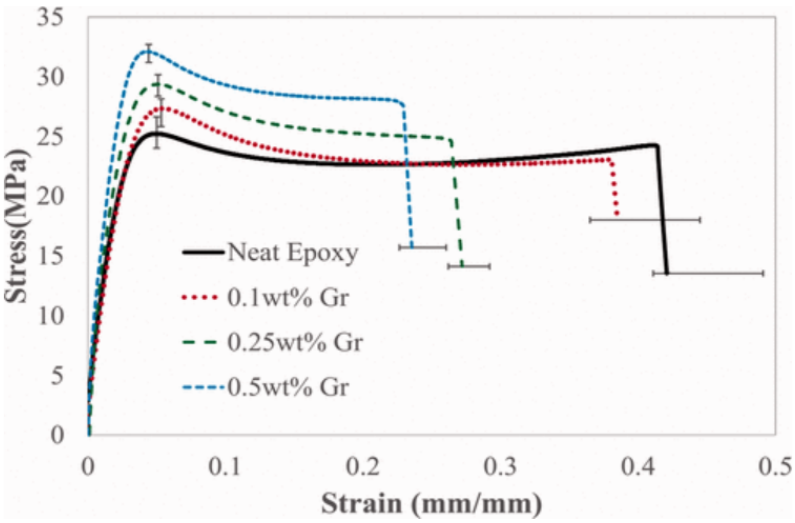

Figure 6.14: Representative stress vs strain curves of neat and reinforced epoxy [36]

A tensile test was conducted to a bulk specimen in AJPU lab, to compare the stress vs strain curves. The thickness of the bulk specimen was 2.1 mm and the width was 8.05 mm, being the cross section of 16.905 mm^2. The temperature was not controlled, the test was performed at room temperature and the loading speed was 1 mm/min, while measuring the strain with an extensometer. The curve is shown in Figure 6.15.

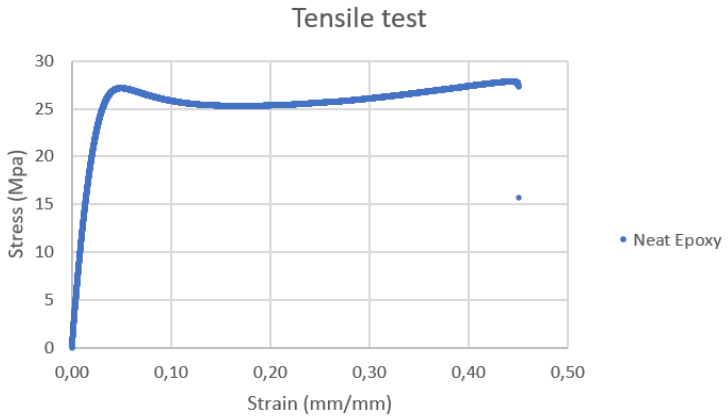

Figure 6.15: Representative stress vs strain curve of neat epoxy

In [36], the maximum stress was about 25 MPa and the strain was about 0.4. The fact that the maximum stress was about 25 MPa, means the mean ultimate load of the neat bulk specimen is equal to 408 N. Therefore, the 220 N load applied during the creep test corresponds to 54% of the neat epoxy ultimate strength. However, the tensile test performed in AJPU lab displayed a maximum stress of about 27.85 MPa and a total strain of 45%, meaning the mean ultimate load of the neat bulk specimen is 470.8 N. The 220 N constant load level during the creep test corresponds to 47% of the epoxy ultimate strength. In Figure 6.16, the neat epoxy creep curve for an applied load of 150 N, which corresponds to 37% of the bulk specimen's ultimate load is displayed. The creep strain is far inferior to the 220 N curve, being the strain after 5000 s of approximately 0.14, and since the ultimate load of the manufactured specimen is 470.8 N instead of 408 N, this might provide an explanation on the difference between the creep curves produced in the developed machine and the ones in [36]. However, once the adhesive plates were not distinguished in the cutting process, there is no accurate way of knowing which adhesive plate's specimens possess the 470.8 N mean ultimate load.

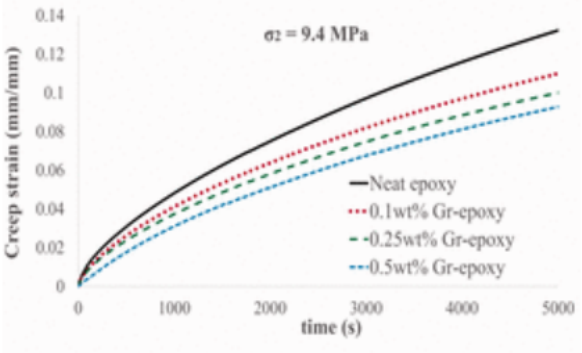

Figure 6.16: Creep strain diagram of the neat and graphene-reinforced epoxy for 150 N [36]

In conclusion, the machine was able to exert a precise load, while maintaining it rather constant during the adhesive creep tests. More so, it showed

the capability to repeat that process in all tests above described. The load factor is the one that can be controlled and both stations performed well in that regard. As for the reliability, the tests are inconclusive. Due to the plates being manufactured in different occasions and, possibly, acquiring different properties and strength, due to the uncertainty regarding the specimens' origin, the different tensile strength between the adhesive bulk specimens in previous studies and the one test in AJPU's laboratory and the incapability of testing the adhesive specimens in other machine, it is difficult to draw conclusions about whether the performed tests are reliable and accurate regarding the creep behaviour. Still, it was previously proven the machine's reliability in providing accurate creep behaviour results when compared to a separate machine, using the polymer specimens and it still provided three very similar creep curves for the adhesive specimens. Therefore, it can be concluded that overall (regarding both polymer and adhesive creep tests) the machine is reliable and produces accurate curves that reflect the real creep phenomenon that these samples are subjected to.

Chapter 7
Conclusion

This chapter summarizes the main conclusion of this dissertation, reporting the objectives achieved and addressing the possible future improvements to be implemented in the system.

7.1 Conclusion

The mechanical design and the pneumatic and electric circuits were revised. The pneumatic circuit was reorganized, corrected and implemented in all three stations. The electric circuit was improved: the damaged equipment was replaced or repaired, some connections were altered and the signal conditioning board 2 was manufactured and implemented, allowing the calibration of all three cylinder's encoders and providing the necessary electric connections in order to all stations become functional. The electrical cabinet is therefore complete, as it contains every component and connection necessary to control the multi-station creep machine.

The software was programmed for all three stations in such way that they were able to perform independent and simultaneous creep testing, without influencing one another, between 100 N and 2800 N. The DAQ connections were established and proven to work correctly with the transducers' measurement alterations. All three stations were also able to record data independently regarding the time, measured load, desired load and displacement as well as identify the cause that ended each creep test. The emergency conditions proved to work and guarantee the user's safety. A debugging panel was implemented to facilitate the discovery of errors or malfunctions of the program by the user. A post-processing interface was designed to facilitate and automate data analysis, providing the user almost instant results about the behaviour of the machine during the creep tests.

All software was verified in terms of functionality and, in some cases, internal structures, which proved that the software was working as intended. The hardware was also put to test, using a secondary program that allowed finding and locating some hardware and connecting errors as well as testing and saving the transducers' behaviour. The Stations 1 and 3 were also put to test, verifying the capability of maintaining a constant load over large periods

of time as well as the response in terms of pressure when the two stations were working asynchronously. Such results were deemed good, having in mind that the VPPX valve is working, for now, in internal mode.

Lastly, both stations performed creep tests, using polymer and adhesive specimens and comparing the results between stations, to other machines and to previous studies about the materials. The results met the expectations, once both stations were able to repeat the load conditions with good precision and accuracy and display similar results to the creep tests performed in other machine and although it was not similar to the ones recorded in previous studies, there were a lot of uncontrolled variables that turn the results inconclusive. However, based on the results obtained in the polymer creep tests and the repeatibility in the adhesive ones, the machine can be validated in terms of performance.

Part of this dissertation was included in the paper: G. N. Bezerra, A. M. Lopes, C. M. da Silva, L. F.M. da Silva "Development of a Multi-station Creep Machine for Adhesive Joint Testing", Journal of Testing and Evaluation, submitted March 12, 2021.

7.2 Future Work

The software and hardware validation tests that were conducted to Stations 1 and 3 should be conducted to Station 2. After, Station 2 should perform some creep tests similar to the ones already performed by Stations 1 and 3 to compare the results and assess the reliability, repeatability and accuracy of Station 2. Also, the pressure influence tests should be repeated with all stations active.

The VPPX valves should be changed from internal mode to external mode, enhancing the performance of the machine during the creep tests and, if AJPU desires, allowing the machine to be able to also perform relaxation tests by adding and changing some code mainly in the "Test in Progress" state of the program. Also, a filter should be implemented to reduce noise effects.

Post-processing interface can also be added with some features according to AJPU needs like the dimension of the specimen in order to analyze the creep tests in terms of stress and strain.

At last, a thermal chamber, which has already been designed, should be manufactured and assembled in order to allow creep testing at different temperatures but also to actively control the temperature during the creep testing and keep it constant.

References

[1] L. F. Da Silva, A. Öchsner, and R. D. Adams, Handbook of adhesion technology. Springer Science & Business Media, 2011.

[2] W. Lees, Adhesives in Engineering Design. Springer, 1984.

[3] H. M. Freire, "Desenvolvimento de um dispositivo experimental para medir a resistência à fluência de ligações adesivas," Master's thesis, MIEM, 2015.

[4] L. P. L. Pina, "Development of a multi-station creep testing machine for adhesive joints," Master's thesis, MIEM, 2016.

[5] E. D. R. Silva, "Development of a three-station creep machine for adhesive joints," Master's thesis, MIEM, 2018.

[6] D. Packham, In Handbook of adhesion second edition. Wiley Online Library, 2005.

[7] M. Miravalles, "The creep behaviour of adhesives," Master's thesis, Chalmers University of Technology, 2007.

[8] A. J. Kinloch, Adhesion and adhesives: science and technology. Springer Science & Business Media, 2012.

[9] L. F. M. d. Silva, Comportamento mecânico dos materiais. Porto: Publindústria, 2012.

[10] "Creep test." https://www.instron.us/en-us/our-company/library/glossary/c/creep-test. Accessed on November 2020.

[11] L. F. Da Silva, D. A. Dillard, B. Blackman, and R. D. Adams, Testing adhesive joints: best practices. John Wiley & Sons, 2012.

[12] INSTRON, "Multi Station systems 5900 Series," 2012.

[13] INSTRON, "Bluehill® Universal Software," 2012.

[14] Zwick Roell, "Kappa Multistation Creep Machine Series," 2012.

[15] Zwick Roell, "TestXpert III Multistation Software," 2012.

[16] Festo, “Standard cylinders DDPC, integrated displacement encoder,” 2017.

[17] Festo, “One-way flow control valves,” 2017.

[18] Festo, “Solenoid valves VUVS / valve manifold VTUS,” 2017.

[19] Festo, “Proportional pressure regulators VPPX,” 2017.

[20] Festo, “Service unit combinations MSB, MS series,” 2017.

[21] AEP Transducer, “TS - TSA Load Cell,” 2018.

[22] AEP Transducer, “TA4/2 Analogue Transmitter,” 2012.

[23] Festo, “DADE Measured Value Converter,” 2015.

[24] Festo, “Proximity sensors SMT / SME-8, for T-slot,” 2018.

[25] National Instruments, “What Is Data Acquisition?,” 2018.

[26] National Instruments, “NI 6010 Specifications,” 2005.

[27] National Instruments, “NI 6703/6704 Specifications,” 2012.

[28] C. Elliott, V. Vijayakumar, W. Zink, and R. Hansen, “National instruments labview: A programming environment for laboratory automation and measurement,” JALA: Journal of the Association for Laboratory Automation, vol. 12, no. 1, pp. 17–24, 2007.

[29] “What is LabVIEW?.” https://www.electronics-notes.com/articles/test-methods/labview/what-is-labview.php. Accessed on October 2020.

[30] M. Ramalho, “Programação básica de LabVIEW,” Instituto Superior Técnico, 2012.

[31] “Basic concepts of LabVIEW?.” https://www.ni.com/getting-started/labview-basics/pt/environment. Accessed on October 2020.

[32] “Application design patterns: State machines.” https://www.ni.com/en-us/support/documentation/supplemental/16/simple-state-machine-template-documentation.html. Accessed on December 2020.

[33] M. L. Bors, “What is a finite state machine?.” https://medium.com/@mlbors/what-is-a-finite-state-machine-6d8dec727e2c. Accessed on October 2020.

[34] R. Bitter, T. Mohiuddin, and M. Nawrocki, LabVIEW: Advanced programming techniques. CRC press, 2017.

[35] Gunt, “Wp 600 experimental unit,” 2018.

[36] A. Khabaz-Aghdam, B. Behjat, L. F. da Silva, and E. Marques, "A new theoretical creep model of an epoxy-graphene composite based on experimental investigation: effect of graphene content," Journal of Composite Materials, vol. 54, no. 18, pp. 2461–2472, 2020.